WAVE EQUATION ANALYSIS OF PILE DRIVING IN GRAVEL

A Thesis

by

WILLIAM DIETERICH LAWSON

Submitted to the Graduate College of
Texas A&M University
in partial fulfillment of the requirements for the degree of

MASTER OF SCIENCE

December 1984

Major Subject: Civil Engineering

WAVE EQUATION ANALYSIS OF PILE DRIVING IN GRAVEL

A Thesis by

by

WILLIAM DIETERICH LAWSON

Approved as to style and content by:

Jean-Louis Briaud
(Co-Chairman of Committee)

Lee L. Lowery, Jr.
(Member)

Mike E. James, Jr.
(Co-Chairman of Committee)

T. J. Hirsch
(Head of Department)

Claude L. Gibson
(Member)

December 1984

ABSTRACT

Wave Equation Analysis of Pile Driving

in Gravel (December 1984)

William Dieterich Lawson, B.S., Texas A&M University

Co-Chairmen of Advisory Committee: Dr. Jean-Louis Briaud
Dr. Mike E. James, Jr.

This thesis presents a wave equation analysis of selected test piles driven at the replacement Lock & Dam No. 26 site on the Mississippi River; the soil is predominately coarse sand and gravel. The fundamental analysis procedure involves varying the soil damping parameter J to match measured static soil resistance and blowcount records. The analysis uses quake values determined by drawing a secant through a point corresponding to 25% of the ultimate load on the load-deflection curves. For each selected pile, the J value that best correlates ultimate static resistance of the time of driving (calculated by the wave equation) and the measured ultimate static resistance from the load tests is zero. The analysis includes the effects of residual stresses; for the one pile which was load-tested in tension, wave equation-calculated residual point load closely matches the measured value. Dynamic pile driving formulas give conservative results in comparison to the load test ultimate resistance values. As background information, this thesis presents wave equation theory, E.A.L. Smith's finite difference solution, an in-depth review of available wave equation computer programs, and a literature review focusing on static and dynamic computer soil models and their accompanying parameters.

ACKNOWLEDGMENTS

As an individual deeply interested in structures and their supporting foundations, I have discovered that writing a thesis is much like the construction of a building or a dam - the foundation must be sound for the structure to survive. This acknowledgment describes my foundation - the sound basis of support I have had while writing this thesis.

The most stable and sure factor in my life is the living Word of God - personified in the man Jesus Christ. His sovereignty and His abiding love gave me the perspective and endurance necessary to finish this thesis. Since Christ is my foundation, and the foundation is laid first, I acknowledge Him - at the beginning - as the very beginning of this work.

Many individuals also supported me while working on this thesis. Special thanks to Chuck Fernald, Steve Grant, Kendall Gurry, Kim Musial, Chris Cook, Jodie and Steve Robinson, Carla and Craig Evans, Furm and Winnie Southern, Leo and Frances Schneider, Bob and Melody Bruner, and my family for their prayers, encouragement, friendship, and love. Extra special thanks to both Shelley Stoffels and Larry Tucker for their unselfish help. A special thank you to Debbie Moy for more things than I know how to say. Also, thank you to Dr. Howard Furr and Dr. Harry Coyle for the benefit of their experience and for their encouragement.

My committee, Drs. Jean-Louis Briaud, Mike James, Claude Gibson, and Lee Lowery, provided excellent guidance and instruction in addition to being an extensive source of technical information. I am deeply

grateful to them. Also, thank you to the many individuals who contributed to this project by providing copies of their dissertation, articles, or technical information. Special thanks to Joy Taylor for the time and care she used in typing this thesis.

Without the strong foundation of support these people provided, I could not have completed this thesis. I warmly and sincerely thank you all.

TABLE OF CONTENTS

	PAGE
ABSTRACT	iii
ACKNOWLEDGMENTS	iv
TABLE OF CONTENTS	vi
LIST OF FIGURES	viii
LIST OF TABLES	xi
CHAPTER I. INTRODUCTION	1
CHAPTER II. WAVE EQUATION THEORY	3
CHAPTER III. SMITH'S COMPUTER SOLUTION	8
CHAPTER IV. WAVE EQUATION COMPUTER PROGRAMS	15
Introduction	15
TAMU Programs	16
CRWU Programs	19
ILLINOIS Program	21
DUKE Programs	22
U.T. Programs	22
Raymond Company Program	23
Laboratoire Central des Ponts et Chaussees Program	23
HBG Program	24
Summary	25
CHAPTER V. LITERATURE REVIEW	26
Uses of the Wave Equation	26
Residual Stress Effects	27
Dynamic Field Measurements	29
Computer Soil Models	31
Static Load-Deformation Behavior Models	32
Quakes	40
Dynamic Soil Behavior Models	46
Smith Damping	49
Summary	50
CHAPTER VI. LOCK & DAM NO. 26: PROJECT DESCRIPTION AND ANALYSIS DATA	53
Project Description	53
The Test Site	56
Soil Description	56

TABLE OF CONTENTS (Continued)

	Page
In Situ Tests	56
Pile Load Test Data	71
Pile Driving Data	95
CHAPTER VII. LOCK & DAM NO. 26: WAVE EQUATION ANALYSIS	104
Objectives	104
Determination of Quake and Damping - Overview	104
Ultimate Static Resistance	105
Selection of Quakes	106
Matching FMAX	111
Developing the Ultimate Static Resistance versus Blowcount Curves	113
Results	115
Discussion	126
Residual Stress Analysis	129
Dynamic Pile-Driving Formulas	136
Summary	138
CHAPTER VIII. CONCLUSIONS	140
Conclusions	140
Recommendations for Further Study	141
REFERENCES	142
APPENDIX I. - PILE TELLTALES DATA	147
VITA	159

LIST OF FIGURES

FIGURE		PAGE
1.	Discrete Element Idealization of the Hammer and Pile	9
2.	Static and Dynamic Load-Deformation Models	12
3.	The Residual Stress Phenomenon	28
4.	Typical Load-Deformation Curve from a Static Load Test	33
5.	Generalized Soil Resistance Model	34
6.	Hyperbolic Soil Resistance Model	36
7.	Bilinear-Elastic/Plastic Soil Resistance Model	37
8.	Linear-Elastic/Plastic Soil Resistance Model	38
9.	Soil Loading Versus Deformation Curves	44
10.	Location of the New Lock & Dam No. 26	54
11.	Phase I of Construction at Lock & Dam No. 26	55
12.	Location of Pile Groups During Phase I of Construction	57
13.	In Situ Test Boring Locations for Pile Group 1	58
14.	In Situ Test Boring Locations for Pile Group 2	59
15.	Location of Test Piles in Pile Group 1	60
16.	Location of Test Piles in Pile Group 2	61
17.	Soil Boring Log for Boring No. B-3	62
18.	Soil Boring Log for Boring No. B-19	64
19.	Soil Boring Log for Boring No. B-21	66
20.	Soil Boring Log for Boring No. B-20	68
21.	Gradation Band of Sieve Analysis Test	70
22.	Standard Penetration Test Results Obtained from Borings at Lock & Dam No. 26	72

LIST OF FIGURES (Continued)

FIGURE		PAGE
23.	Cone Penetrometer Data: Tip Resistance Versus Depth	73
24.	Cone Penetrometer Data: Sleeve Friction Versus Depth	74
25.	Pressuremeter Data: Net Limit Pressure Versus Depth for Pile Group 1	75
26.	Initial Pressuremeter Modulus Versus Depth for Pile Group 1	76
27.	Reload Pressuremeter Modulus Versus Depth for Pile Group 1	77
28.	Pressuremeter Data: Net Limit Pressure Versus Depth for Pile Group 2	78
29.	Initial Pressuremeter Modulus Versus Depth for Pile Group 2	79
30.	Reload Pressuremeter Modulus Versus Depth for Pile Group 2	80
31.	Load Versus Pilehead Movement for Pile 1-3A	83
32.	Load Versus Pilehead Movement for Pile 1-6	84
33.	Load Versus Pilehead Movement for Pile 1-9	85
34.	Load Versus Pilehead Movement for Pile 2-5	86
35.	Point Load Versus Point Deflection for Pile 1-3A	87
36.	Point Load Versus Point Deflection for Pile 1-6	88
37.	Point Load Versus Point Deflection for Pile 1-9	89
38.	Point Load Versus Point Deflection for Pile 2-5	90
39.	Friction Load Versus Average Deflection for Pile 1-3A	91
40.	Friction Load Versus Average Deflection for Pile 1-6	92

LIST OF FIGURES (Continued)

FIGURE		PAGE
41.	Friction Load Versus Average Deflection for Pile 1-9	93
42.	Friction Load Versus Average Deflection for Pile 2-5	94
43.	ICE 640 Diesel Pile Driving Hammer - Schematic Drawing	97
44.	Driving Record for Pile 1-3A	100
45.	Driving Record for Pile 1-6	101
46.	Driving Record for Pile 1-9	102
47.	Driving Record for Pile 2-5	103
48.	Ultimate Static Soil Resistance Versus Blowcount for Selected Piles at Lock & Dam No. 26	108
49.	Determination of 25% Secant Quake Values	109
50.	RUT Versus N for Pile 1-3A Using 50% Secant Quakes.	116
51.	RUT Versus N for Pile 1-3A Using 25% Secant Quakes.	118
52.	RUT Versus N for Pile 1-9 Using 25% Secant Quakes	122
53.	RUT Versus N for Pile 2-5 Using 25% Secant Quakes	124
54.	Residual Point Load Results for Pile 1-3 Using 50% Secant Quakes	131
55.	Residual Point Load Results for Pile 1-3 Using 25% Secant Quakes	134

LIST OF TABLES

TABLE		PAGE
1.	Summary of Quake Values for Cohesionless Soils	42
2.	Summary of Smith Damping Values for Cohesionless Soils	51
3.	Lock & Dam No. 26 Pile Load Test Summary	81
4.	ICE 640 Diesel Pile-Driving Hammer Data	96
5.	Dynamic Field Measurements from the Pile Driving Analyzer	99
6.	Ultimate Static Soil Resistance and Corresponding Blowcount Data	107
7.	Quake Values Used for this Analysis	110
8.	RUT and Blowcount Results for Pile 1-3A *Using* 50% Secant Quakes	117
9.	RUT and Blowcount Results for Pile 1-3A Using 25% Secant Quakes	119
10.	RUT and Blowcount Results for Pile 1-6 Using 25% Secant Quakes	120
11.	RUT and Blowcount Results for Pile 1-9 Using 25% Secant Quakes	123
12.	RUT and Blowcount Results for Pile 2-5 Using 25% Secant Quakes	125
13.	Ultimate Static Soil Resistance Calculated by the Wave Equation for Zero Damping	127
14.	Residual Point Load Results for Pile 1-3 Using 50% Secant Quakes	132
15.	Residual Point Load Results for Pile 1-3 Using 25% Secant Quakes	135
16.	Dynamic Pile Driving Formula Results	139

CHAPTER I

INTRODUCTION

The advent of high-speed digital computers thrust the state-of-the-art of dynamic pile driving analysis far beyond the capabilities of simple pile driving formulas. The basis for those formulas is the incorrect assumption that pile driving obeys the theory of Newtonian impact; rather, pile driving is a problem of longitudinal wave transmission (11). The one-dimensional wave equation more properly models dynamic behavior of a pile during driving, and high-speed digital computers enable engineers to obtain practical solutions to the problem.

E.A.L. Smith (43) published the original paper on the subject in 1960. He outlined the numerical method of the wave equation computer program and discussed physical conditions that must be taken into account in the solution. He also presented the mathematical equations for the solution and set up the computer routines. Smith's paper is the basic reference for practically every wave equation computer program in use today.

Proper understanding of the wave equation method necessitates the derivation of the second-order partial differential equation (the wave equation) with assumptions, and also Smith's numerical finite difference solution. In addition, the report includes a comprehensive presentation of the various wave equation computer programs. Since

---

The style and format of this thesis follows that used by the Journal of the Geotechnical Engineering Division, American Society of Civil Engineers.

pile driving history is not germane to this report, it is not in the text; Chan et al. (7) adequately describe the history of pile driving.

The literature review focuses on recent developments in the wave equation method of pile driving analysis. Specifically, the literature review emphasizes published work describing static and dynamic soil behavior models used in various computer programs. The literature review also includes a comprehensive presentation of the quake and damping parameters for cohesionless soils.

The objective of the analysis portion of this research is to determine quake and damping parameters for gravel. The Corps of Engineers' project, Lock & Dam No. 26, provided the necessary data for the analysis. This report briefly describes the Lock & Dam No. 26 project and the site. It also provides all pertinent hammer, pile, and soil data required for the analysis, including the pile load test data.

The wave equation method was the exclusive research tool used for the analysis. The report describes the analysis in detail, from selecting quake values to developing RUT versus N curves. The final sections of the report recommend values for the quake and damping parameters and describe the residual stresses portion of the analysis. Selected pile driving formulas are also compared with the wave equation and load test results. The report summarizes findings and points out areas for further research.

CHAPTER II

WAVE EQUATION THEORY

The wave equation describes how waves propagate from one point to another. In the pile driving problem, the wave equation illustrates wave action produced by a force suddenly applied at one end of a long object. Holloway (after Timoshenko) derives the one-dimensional wave equation in detail based upon the equilibrium equation of motion at a point on a rod (27). The following is an abbreviated version of his work.

In terms of stresses, the wave equation is:

$$A \frac{\partial \sigma_x}{\partial x} - R = \rho A \frac{\partial^2 u}{\partial t^2} \tag{1}$$

where $\sigma_x = \sigma_x(x,t)$; stress at a point on the rod, F/L^2
where F = force and L = length

x = coordinate location of a point along the rod

A = A(x); cross-sectional area, L^2

R = R(x,t); element resistance force, F/L

$\rho = \rho(x)$, mass density, M/L^3, where M = mass

u = u(x,t); element displacement, L

t = time

If the material is assumed to be a linearly elastic solid subject only to infinitesimal strains, Hooke's stress-strain law for small strain theory applies:

$$\sigma_x = E \, \epsilon_x = E \frac{\partial u}{\partial x} \tag{2}$$

where $E = E(x)$, Young's modulus, F/L^2

ε_x = strain at a point along the rod

Imposing these assumptions on Eq. 1 gives the wave equation as a function of the unknown displacement $u(x,t)$:

$$A \frac{\partial}{\partial x} \left(E \frac{\partial u}{\partial x}\right) - R = \rho A \frac{\partial^2 u}{\partial t^2} \tag{3}$$

For a freely suspended rod, the resistance term vanishes and the partial differential equation becomes:

$$\frac{E}{\rho} \frac{\partial^2 u}{\partial x^2} = \frac{\partial^2 u}{\partial t^2} \tag{4}$$

which is the most common form of the one-dimensional wave equation. The quantity E/ρ is usually shown as C^2; C is the velocity of wave propogation in the material.

Solution of a particular problem requires both initial conditions and boundary conditions. For the more general form of Eq. 3, the initial conditions are:

$$u(x,t) = u_o(x) \text{ at } t = t_o$$
$$\frac{\partial u}{\partial t}(x,t) = V_R(x) \text{ at } t = t_o$$
$$R(x,t) = R_o(x) \text{ at } t = t_o$$

where

o(subscript) = initial value with respect to time.

V_R = ram impact velocity.

The boundary conditions are:

$$u(x,t) \text{ or } \frac{\partial u}{\partial x}(x,t) \quad \text{at} \quad x=0$$
$$u(x,t) \text{ or } \frac{\partial u}{\partial x}(x,t) \quad \text{at} \quad x=L$$

Application of these initial and boundary conditions satisfies a necessary condition for the existence of a unique solution. This is an "exact" solution inasmuch as "exact" solutions are possible.

Application of wave equation theory is valid only when the application satisfies the theory's underlying assumptions; therefore, the assumptions are stated here for emphasis (27).

(1) Hooke's stress-strain law for small strain theory is incorporated in Eqs. 3 and 4. As long as the rod is stiff relative to the stress level, this assumption causes little inaccuracy. If the rod is relatively soft, three-dimensional effects and geometric nonlinearity could cause considerable errors.

(2) The dynamic resistance to motion due to external forces may be a complex function of space- and time-dependent variables. For example, the resistance at a point along the rod may depend on both the displacement and time derivatives of displacement at that point.

(3) Determining material behavior parameters is not necessarily easy. For example, extensive research has been conducted to describe soil-pile interaction behavior, yet soil models are

still the most variable facet of the pile driving solution.

Cummings (11) also states the assumptions on which wave equation theory is based. His presentation describes the physical aspects of the pile driving solution. The assumptions are:

(1) The sides of the pile are free and there is no side friction to affect stress waves running up and down the pile.

(2) Stress waves in the hammer may be neglected.

(3) There are no flexural vibrations of the pile.

(4) The pile behaves as a linearly elastic rod.

(5) The hammer strikes directly on the head of the pile, and the surfaces of contact are two ideal smooth parallel planes.

(6) The lower end of the pile is fixed.

Assumption 1 implies that skin friction reduces the amplitudes of stress waves traveling in the pile and therefore reduces the stresses themselves. Propagation losses in the pile also reduce stresses. Consequently, neglecting skin friction and propagation losses results in higher theoretical stresses than actual stresses.

Assumption 2 does not produce any significant error for steam and drop hammers since the hammer is usually a heavy block of iron or steel, and, for all practical purposes, can be modeled as a rigid body. This may not be the case for diesel hammers, however.

Concerning assumption 3, Cummings demonstrated that flexural buckling of a foundation pile under static loads is a remote possibility even in very soft soils. The same comment applies to dynamic loads as long as the pile and hammer are in good alignment and the force of the hammer blow is concentric with the longitudinal axis of

the pile. Typically, neglecting flexural vibrations introduces no serious error when applying the theory of longitudinal impact to pile driving.

Assumption 4 is reasonably valid for most types of piles that are used commercially. Composite piles or any other kinds of piles composed of two or more separate sections do not satisfy this assumption. The transmission of stresses across the joints of such piles is a special problem.

Assumption 5 applies since almost all practical pile driving is done with some sort of cushion or driving block between the hammer and the pile head. The cushion reduces stresses so that actual stresses are less than those given by the theory.

As far as assumption 6 is concerned, the point of the pile is hardly ever fixed in the sense required by theory. The resistance at the pile point depends on the nature of the soil at the pile point. Soils data remains the most variable factor in the wave equation solution.

The one-dimensional wave equation is the mathematical representation of an idealized, classical mechanics problem. E.A.L. Smith (44) commented on the solution:

> "For very simple cases, as when a known force is suddenly applied at one end of a uniform steel rod, the equation can be solved by ordinary calculus. But when the equation is complicated by considerations of the actions of the ram, the cap block, the pile, and the ground, the problem becomes so difficult that no one has been known to solve it."

CHAPTER III

SMITH'S COMPUTER SOLUTION

In 1955, Smith (42) introduced an approximate numerical (finite difference) technique for solving the problem of longitudinal impact in an elastic rod. In 1960, he published a paper which dealt exclusively with the application of his numerical technique to the pile driving problem. The following presentation of the numerical solution is from Smith's paper (43) with notation slightly modified by Samson et al. (41).

Smith derived five governing equations from the elementary laws of physics. The assumptions are that all springs are perfectly elastic and that the pile is represented typically as shown in Fig. 1. The equations are:

$$D(m,t) = D(m,t-1) + 12\Delta t V(m,t-1) \quad . \quad . \quad . \quad . \quad . \quad . \quad . \quad . \quad . \quad . \quad (5)$$

$$C(m,t) = D(m,t) - D(m+1,t) \quad . \quad . \quad . \quad . \quad . \quad . \quad . \quad . \quad . \quad . \quad . \quad . \quad (6)$$

$$F(m,t) = C(m,t)\, K(m) \quad . \quad . \quad . \quad . \quad . \quad . \quad . \quad . \quad . \quad . \quad . \quad . \quad . \quad . \quad (7)$$

$$R(m,t) = [D(m,t)-D'(m,t)]\, K'(m)[1+J(m)V(m,t-1)] \quad . \quad . \quad . \quad (8)$$

$$V(m,t) = V(m,t-1)+[F(m-1,t)-F(m,t)-R(m,t)]\, \frac{g\Delta t}{W(m)} \quad . \quad . \quad . \quad (9)$$

where

( ) = functional designation

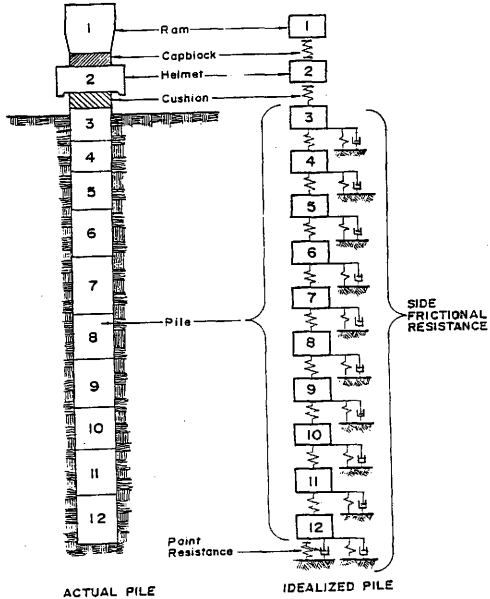

FIG. 1. - Discrete Element Idealization of the Hammer and Pile (After Ref. 43)

m = element number

t = number of time interval

Δt = size of time interval (T), where T = time

C(m,t) = compression of internal spring m in time interval t (L), where L = length

D(m,t) = displacement of element m in time interval t (L)

D'(m,t) = plastic displacement of external spring m in time interval t (L)

F(m,t) = force in internal spring m in time interval t (F), where F = force

g = gravitational acceleration (L/T^2)

J(m) = damping constant of soil at element m (T/L)

K(m) = spring constant associated with internal spring m (F/L)

K'(m) = spring constant associated with external spring m (F/L)

R(m,t) = force exerted by external spring m on element m in time interval t (F)

V(m,t) = velocity of element m in time interval t (L/T)

W(m) = weight of element m (F).

The internal spring constant K(m) satisfies the assumption that all springs must be perfectly elastic (which implies no internal damping). The assumption is valid for typical pile segments. The capblock and cushion block, however, do have internal damping, and Smith developed special relationships to account for it. Instead of

Eq. 7, he used the following equation:

$$F(m,t) = \frac{K(m)}{[e(m)]^2} C(m,t) - \left(\frac{1}{[e(m)]^2} - 1\right) K(m)\ C(m,t)_{max} \qquad (10)$$

where

$e(m)$ = coefficient of restitution of internal spring m

$C(m,t)_{max}$ = temporary maximum value of $C(m,t)$

The mathematical expression for the external spring constant K'(m) (see Fig. 2(a)) is:

$$K'(m) = \frac{R_u(m)}{Q(m)} \qquad (11)$$

where

$Q(m)$ = quake, the maximum elastic deformation allowed for external spring m (L)

$Ru(m)$ = ultimate ground resistance, or the load at which the external spring m behaves in a purely plastic manner (F)

The computations proceed as follows:

1. Determine the initial velocity of the ram from properties of the pile driver. Initialize other time dependent quantities to zero.
2. Calculate displacements D(m,1) by Eq. 5. Note that V(1,0)

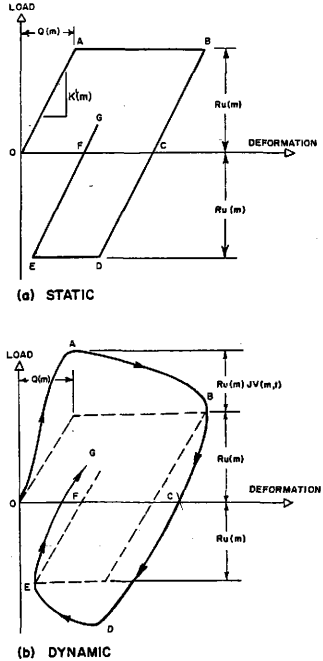

FIG. 2. - Static and Dynamic Load-Deformation Models (after Ref. 43)

is the initial velocity of the ram.

3. Calculate compressions C(m,1) by Eq. 6.
4. Calculate internal spring forces by Eq. 7 or Eq. 10, as appropriate.
5. Calculate external spring forces R(m,1) by Eq. 8.
6. Calculate velocities V(m,1) by Eq. 9.
7. Repeat the cycle for successive time intervals.

In Eq. 8, the plastic deformation D'(m,t) follows Fig. 2(a) and is determined by special routines. For example, when D(m,t) is less than Q(m), D'(m,t) is zero; when D(m,t) is greater than Q(m) along line AB (see Fig. 2(a)), D'(m,t) equals D(m,t) - Q(m).

Smith noted that Eq. 8 produces no damping when D(m,t) - D'(m,t) equals zero. He suggested an alternate equation be used when D(m,t) first equals Q(m):

$$R(m,t) = [D(m,t) - D'(m,t)]\, K'(m) + J(m)Ru(m)\, V\,(m,t-1) \qquad (12)$$

The pile point is a special case. When m=p, where p is the number of the last element of the pile, K(p) is the point soil spring and J(p) is the point soil damping constant. Fig. 2(b) shows dynamic load-deformation behavior. Eq. 8 produces the behavior shown by path OABCDEFG in Fig. 2(b). Since the soil spring at the pile point cannot exert tension, the point soil resistance follows path OABC in Fig. 2(b).

After many cycles of computation, the pile segments reach their maximum downward movement and rebound upward. Numerical integration

typically halts, and the program calculates permanent set; permanent set (downward displacement) equals the maximum displacement minus quake. The permanent set of the pile point D(p) due to the ram blow is equal to OC on Figs. 2(a) and 2(b).

The end result of a wave equation analysis is a record of the response of each of the model segments to the hammer blow. In addition to calculating the permanent set, the program keeps a record of the peak compressive and tensile stresses occurring within each of the pile springs. These peak forces divided by the corresponding pile area equal the peak dynamic pile stresses.

Often, engineers perform the above calculations for several values of total static soil resistance and develop classic soil resistance vs. blow count (RUT vs. N) graphs.

CHAPTER IV

WAVE EQUATION COMPUTER PROGRAMS

Introduction

The preceding solution of the elemental (wave) equations of motion for discrete element models is the basis for practically all wave equation computer programs in use today. Researchers at five universities and three private firms have made basic contributions to the development of wave equation technology, either by developing wave equation computer programs or by determining material behavior characteristics for input in the programs, or both. The various computer programs, by source, are:

Texas A&M University (TAMU)

- FHWAWAVE
- TTI
- OCEANWAVE
- TIDYWAVE
- MICROWAVE

Case Western Reserve University (CRWU)

- WEAP
- CAPWAP
- SWEAP

University of Illinois (ILLINOIS)

- DIESEL 1

Duke University (DUKE)

DUKFOR

PSI

University of Texas (U.T.)

DRIVE 7

DRIVE 10

Raymond Company Program

Laboratoire Central des Ponts et Chaussees

BATLAB

HBG (Hollandsche Beton Groep n.v.)

PILEWAVE

The following descriptions of all computer programs provide basic background information. From a user/buyer standpoint, they focus on program capabilities, special applications, and program limitations, as applicable.

TAMU Programs

All TAMU programs use Smith's original algorithm, that is, step-by-step (Euler) integration of the wave equation usually until the pile tip starts to rebound. The solution then halts and pile set per blow is estimated as the maximum tip displacement minus the elastic rebound quake. (Actually, halting the numerical integration

at tip rebound is a money-saving routine built into the programs; the user can continue integration indefinitely and thereby accurately calculate permanent set by simply exercising one of the option capabilities of the program.) Though they all use the same solution algorithm, the programs differ widely in their applications as discussed in the following paragraphs.

FHWAWAVE, written for the Federal Highway Administration (23), is a production version for highway engineers. The user's manual (24) contains numerous example problems and is specifically written for the practicing highway engineer. The program models only a single blow of the hammer. It is formulated to handle drop hammers, both single-acting and double-acting air/steam hammers, and both open-end and closed-end diesel hammers. The program uses Smith's soil model and provides for various soil resistance distributions. All TAMU programs have been criticized for their diesel hammer routines (19, 28). Typically, their routines calculate higher forces delivered to the pile head - and consequently higher pile stresses and larger point displacements - than measurements indicate. Rempe (39) discusses the problem in detail. TAMU researchers were aware of the problem and quantified the discrepancy (34).

TTI has basically the same capabilities as FHWAWAVE. Both programs were written for highway engineers (TTI was written for the Texas Highway Department), and the above description applies.

OCEANWAVE was written by Lowery for a consortium of oil companies (Lee Lowery, Jr., TAMU, personal communication, 7-2-84). OCEANWAVE is a design oriented program and essentially corresponds to FHWAWAVE but with improved input/output capabilities. Other refinements include a

new algorithm to simulate hydraulic hammers (28).

TIDYWAVE was written by Lowery (33), and is, by virtue of an extensive option system, a research oriented version of the wave equation computer program. (The options do not render it impractical for production use, however.) TIDYWAVE contains a parameter variation scheme enabling the engineer to easily determine the sensitivity of the pile driving system to its descriptive parameters. In addition to basic program capabilities (like those in FHWAWAVE), the program includes the following options:

- simulation of limited force or variable force (hydraulic) hammers
- multiple hammer blows, for proper determination of residual stress effects
- long form force vs. time input (when available from field measurements), to eliminate uncertainties caused by the driving hammer and driving accessories
- simulation of hammer located at any point in the pile, i.e. head (normal), butt, midlength, etc.
- inclusion of jacking forces at any point on the pile
- inclusion of a "stinger" or "follower", for offshhore applications
- inclusion of a nonlinear soil resistance model; that is, adequate modeling of any soil load-deformation curve the engineer believes is appropriate
- allowance for different loading and unloading quakes (in Smith's soil model)

- calculation of pile bearing capacity by various pile-driving formulas, for comparison with wave equation solution.

TIDYWAVE's input may be cumbersome for novice users. The option system makes TIDYWAVE the most versatile of TAMU's main-frame computer programs.

MICROWAVE is a new wave equation computer program developed especially for the microcomputer. It mimics FHWAWAVE; that is, the user's manual for FHWAWAVE is applicable to MICROWAVE. Output is in the same form, too. MICROWAVE has a user-interactive data loader and checker (Lee Lowery, Jr., TAMU, personal communication, 7-2-84).

CRWU Programs

WEAP was written by Goble and Rausche (19) for the Federal Highway Administration in an attempt to improve the diesel hammer routine used in the TTI program. WEAP simulates both mechanical and thermodynamic aspects of diesel hammers. The algorithm uses a segmented ram and considers steel on steel impact between the ram and anvil; it also accounts for energy losses at hammer component interfaces. Thermodynamic modeling includes calculating the ram stroke and combustion chamber pressure. WEAP analytically determines the variable energy characteristic of diesel hammers. Numerically, the program uses Newmark-Beta step-by-step integration (based on linear acceleration). WEAP also uses a "predictor-corrector" approach to achieve convergence of both the pile top force and bottom velocity. The program offers two choices for soil damping: (1) standard Smith damping and (2) Case damping, which incorporates the average properties (impedance) of the pile elements. Concerning input

capabilities, WEAP stores a list of hammers on file. To input hammer information, the user need only specify the hammer number. Long form input is also available. WEAP models all conventional hammers but does not model the new hydraulic hammers. Also, WEAP models only a single hammer blow.

CAPWAP (17, 2) makes use of measured force and acceleration records at the pile head to predict the soil resistance distribution mobilized during response to the hammer blow. Essentially, CAPWAP takes the acceleration curve and calculates, with the aid of six operator-controlled variables, a force curve which is matched to the measured force curve. The six variables are side and tip quake, side and tip damping, and load along the pile shaft and at the pile tip. The operator interacts with the computer making several successive runs, each time changing the parameters in an attempt to improve the match between the computed and measured force-time curves. The analysis result is the distribution of mobilized soil resistance -- i.e., the ultimate static bearing capacity and the selection of variables used to achieve the final match. Originally, CAPWAP was fully automated. The automatic computational procedure was reasonably satisfactory for relatively short piles, say, 80 ft (24 m) or less, but when used on long offshore piles the analysis cost became excessive. Consequently, the program was modified to compute resistance forces and their distribution using the interactive mode described above (18). CAPWAP does not take into account residual stresses in its predicted soil distribution.

SWEAP is a limited version of WEAP for use on a minicomputer

(Frank Rausche, Goble and Associates, personal communication, 6-18-84). Published information on the program is very scant; however, Goble (20) indicates that SWEAP is a combination of WEAP and DUKFOR implying the simulation of a multiple blow analysis for inclusion of residual stress effects. According to Dover et al. (13), SWEAP is executed on a microprocessor system that includes a microprocessor unit, an interactive CRT console, a printer, and a plotter. Program software is stored on floppy disks.

ILLINOIS Program

Rempe (39) developed DIESEL 1 in 1975 as part of a comprehensive study of diesel pile-driving hammer performance. He investigated all aspects of diesel pile driving, - that is, the hammer, the accessories, the pile, and the soil; he also studied how the different aspects interact to affect hammer performance, for example, the case of soft-ground driving or battered-pile driving. The result is the rigorous mathematical hammer model of DIESEL 1. This model accurately simulates diesel hammers by properly modeling the entire thermodynamic cycle, realistically approximating the gas force by considering both hammer design features and hammer-pile-soil interaction, using a segmented ram, and providing for damping of spurious oscillations. DIESEL 1 is based on Smith's original algorithm and uses a discrete-element pile representation. No published information is available on program soil models, input, output, or special capabilities.

DUKE Programs

DUKFOR was written by Holloway (26) in order to analyze pile-soil interaction behavior more effectively. The computer code simulates impact pile driving and/or pile load test behavior in a unified approach. DUKFOR analyzes a series of hammer blows, statically equilibrating the forces at the end of each blow and taking into account residual driving stresses. The code provides for either bilinear or hyperbolic static deformation soil behavior. DUKFOR also includes three possible dynamic soil behavior components: no damping, nonlinear viscous damping after Smith, and linear viscous damping. DUKFOR uses Smith's basic discrete element formulation and numerical integration scheme.

PSI (28) is an updated version of DUKFOR developed to accommodate longer piles and to simplify certain analysis inputs. PSI, like DUKFOR, has the capability of performing multiple blow analyses thereby incorporating residual stresses in the solution. The program's primary limitation is the absence of diesel hammer and hydraulic hammer simulators. Work was underway in 1978 to include the special hammer routines in the code; the present status of PSI and DUKFOR was not discussed in more recent literature, however.

U.T. Programs

DRIVE 7, described by Matlock and Foo (36), analyzes the driving of foundation piles by impact or vibration plus a variety of problems dealing with static or dynamic axial loading of bars. A discrete-element mechanical analogue represents the pile member, and a hysteretic, degrading support model describes the nonlinear inelastic

behavior of the soil. DRIVE 7 provides for strength degradation as a function of deflection and of the number of reversals of deflection in the range beyond an initially elastic condition. The code allows for any soil variation with depth. Hammer blows may be applied at any point along the pile length, and the driving system has the capability to include a mandrel or follower in the analysis. DRIVE 7 allows for input of measured force-time data rather than simulating the hammer. The numerical alogrithm employs an implicit (Crank-Nicolson) type solution to maintain stability and accuracy. DRIVE 7 has the capability to simulate multiple hammer blows thereby taking residual stresses into account. The algorithm calculates permanent set based on the complete time history of pile tip movement rather than by maximum displacement minus quake.

DRIVE 10 is an improved version of DRIVE 7 (Dwaine Bogard, Earth Technology Corp., personal communication, 6-20-84). The basic improvement is in the output; otherwise, the two programs are the same. The U.T. programs do not contain diesel hammer or hydraulic hammer simulators.

Raymond Company Program

The Raymond Company program is the program written by E.A.L. Smith. It has been updated somewhat (Paul Engeling, Raymond International, personal communication, 6-18-84), but information on those improvements is not available.

Laboratoire Central des Ponts et Chaussees Program

BATLAB was developed in France by the Laboratoire Central des

Ponts et Chaussees (3). BATLAB differs from other programs in that it contains no hammer model; the user must input a force-time curve (actual or simplified). BATLAB only models, then, the pile and the soil. The authors of BATLAB believe that the numerical integration technique is a very critical aspect of a discrete element solution. They concentrated on developing an integration algorithm which precisely calculates the displacement and velocity history of an element during a time interval at least equal to the time it takes for the stress wave to travel up and down the pile. BATLAB uses Runge-Kutta numerical integration. The soil model is bilinear elastic-plastic with linear damping.

HBG Program

PILEWAVE, written by Voitus van Hamme (50), is the only program based on a solution to the wave equation; all other programs are based on a discrete-element formulation after Smith. Voitus van Hamme contends that his program has important advantages over pile-driving programs based on concentrated masses interconnected by springs. First, force and velocity are always calculated for the same points. Second, phenomena which occur at places where no traction can be sustained (e.g., between a pile and an add-on) can be assessed accurately. Third, the pile driving hammer, even a complicated one, and the pile cap with cushions can easily be incorporated into the system. Fourth, this "solution of the wave equation" theory not only leads to a simple computer program but also provides a much better understanding of what really happens during pile driving. PILEWAVE was originally written to analyze pile driving by the Hydroblok

hammer (31), but versions for conventional steam and diesel hammers are also available. Jansz et al. (31) published results showing a very good comparison between computed and measured force-time curves for the Hydroblok hammer.

Summary

All of the previously described wave equation computer programs, with the exception of the TAMU programs and WEAP, are proprietary in some sense of the word. Either they were developed by a private firm and are not for distribution (e.g. CAPWAP, the Raymond Program), or they were developed at a university but have not been documented in such a way that they would be useful to the public sector (e.g., DIESEL 1).

The various wave equation computer programs have specific applications and are subject to certain limitations. All of them, however, attempt to solve the wave equation numerically, and they are an invaluable tool for pile foundation analysis and design.

CHAPTER V

LITERATURE REVIEW

This chapter reviews current literature on the wave equation method of pile driving analysis. Specifically, it describes various uses of wave equation computer programs, residual stress effects, and dynamic field measurements.

Uses of the Wave Equation

Several "state-of-the-art" summary papers on wave equation analysis of pile driving are available e.g., references (34), (25), (8), (27), (28), (20), and (2). According to Holloway et al. (28), in 1978, wave equation computer programs provided solutions to a number of piling problems including:

(1) Selection of a suitable hammer assembly-pile-soil combination for a particular site.

(2) Minimizing the potential for pile or hammer damage during driving by predicting peak stresses in the system during driving.

(3) Prediction of the ultimate bearing capacity of a single pile based on measured blow counts.

(4) Prediction of driveability of a pile to full penetration, or how much penetration can be obtained with a given hammer-pile-soil system.

More recently, pile driving analysis has evidenced an increased use of dynamic field measurements to improve the quality of the above solutions (20). In addition, dynamic measurements are being used to

test for pile integrity (2), and engineers are considering the importance of residual stresses during pile driving. The following paragraphs describe residual stresses and dynamic measurements inasmuch as they apply to this research project.

Residual Stress Effects

Correct interpretation of pile behavior under axial loads requires proper determination of residual stresses. The residual stress phenomenon arises in a number of ways (4).

During a hammer blow, a pile will first move downward and then rebound and then oscillate around a final position. The pile, in equilibrium, is under a certain point load and a certain friction load, and these loads must cancel out since the load at the pile head is zero. After several blows (when the pile reaches final penetration), the residual load distribution in the pile is as shown on Fig. 3.

During the downward movement of the pile, the pile-soil friction acts upward to resist the penetration of the pile; the point resistance also acts upward. During the rebound phase, the soil under the point pushes the pile up while the pile decompresses elastically. These two components of rebound create enough upward movement to reverse the direction of the pile-soil friction (which now acts downward -- at least in the upper portion of the pile). Equilibrium is reached when enough friction stresses reverse themselves to keep the bottom of the pile stressed against the soil.

The unloading characteristics of the point and friction transfer curves and the elastic characteristics of the pile govern the residual

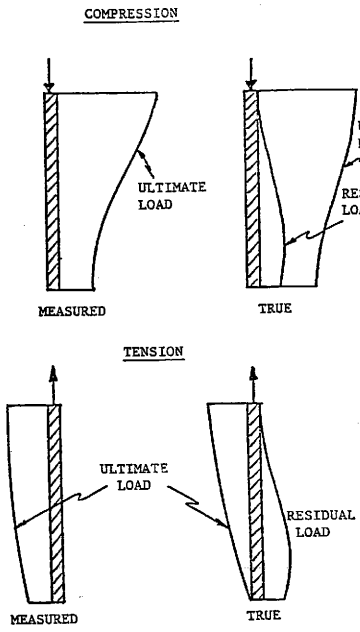

FIG. 3. - The Residual Stress Phenomenon (after Ref. 14)

stress phenomenon. Residual stresses can also be caused by reconsolidation after driving, provided relative movement between the pile and soil occurs. In sands, a significant residual point load can exist because point capacities are large and because the friction transfer curve requires less movement to unload than the point transfer curve requires.

Neglecting residual driving stresses in analyzing pile load tests usually results in (1) overestimating pile shaft capacity, (2) underestimating point capacity, and (3) incorrectly determining the actual resistance distribution at failure (29). Also, neglecting residual stresses in pile driving analyses by performing only a single blow analysis will generally lead to higher predicted blow counts for the same soil resistance. Proper inclusion of residual stresses requires the simulation of 3 to 5 hammer blows (5).

Holloway's program, DUKFOR (26), pioneered the inclusion of residual stress effects in pile driving analyses. DUKFOR models a sequence of hammer blows, statically equilibrating the remaining dynamic forces after each blow. Lowery's program, TIDYWAVE (33), includes a multiple hammer blow routine to allow for inclusion of residual stresses, as does DRIVE 7 (36).

Dynamic Field Measurements

Researchers at Case Western Reserve University developed the most well known system for dynamic measurements, the Case-Goble system (2, 20). The Case-Goble system uses independent measurements of strain and acceleration taken in the field. The strain is directly converted to force, and the acceleration is integrated to obtain the velocity of

the pile. The "Pile Driving Analyzer" system records the measurements. Goble et al. (17) and Authier and Fellenius (2) thoroughly describe the actual system.

The Analyzer calculates three values and prints them out on paper tape. The operator selects the three values from a list of several alternative values, such as impact force, maximum force, and developed energy. Simultaneously with the print-out provded by the Analyzer, an oscilloscope displays traces from pile strain gauge pairs. All measurements are stored on a tape recorder; replaying the tape through the Analyzer simulates original driving. Values that were not selected for print-out the first time through can be obtained in a new output mode.

Dynamic field measurements at the pile head during driving are very desirable since they negate the need for a hammer model in wave equation computer programs. In effect, dynamic measurements remove all uncertainties associated with hammer modeling; the only remaining unknowns in the system are the soil resistance distribution and the soil model parameters.

As previously discussed, CAPWAP uses dynamic measurements to obtain a value of the soil resistance distribution and the soil model parameters. Dolwin and Poskitt (12) discuss a method which also uses dynamic measurements to determine wave equation input parameters. Dolwin and Poskitt's method is a completely automated formulation using a least-squares technique to arrive at the "best" values. These optimization techniques, when coupled with static load test results, provide the best available method of determining soil input parameters for use in wave equation computer programs.

Computer Soil Models

All wave equation computer programs must numerically model the entire pile driving system - - that is, the hammer, the pile, and the soil. Current hammer models adequately simulate the force delivered to the pile head for all hammer types, and force-time data measured at the pile head eliminates any uncertainty in the hammer-capblock-cushion assembly. The pile model is well established and has remained basically the same since Smith first introduced his discrete element idealization. The soil model, however, is another story. Chan et al. (7) discussed rheological soil models:

> "Rheology is the science of deformation and flow ... the goal of rheology is depiction of the deformation of flow resulting from the application of a given force system to a body."

however,

> "the task of determining a rheological model to simulate the complex behavior of soil is generally *far from simple.*"

E.A.L. Smith's rheological soil model satisfies the two basic requirements outlined by Chan:

1. Under an instantaneously applied load (dynamic load), the model should undergo an instantaneous deformation and approach a limiting value.
2. The greater the rate of loading, the steeper the curve in the load-deformation diagram.

There are two main objections to Smith's model, however. One is that

the model is linear. The second objection is that the response of the model is reversible. It is possible to improve the similitude of action of the model in these two respects, but with such alteration the mathematics becomes rapidly more complex. Chan adopted Smith's two-element model as a compromise between the conflicting requirements of realism and simplicity.

Several computer programs have "complicated the mathematics" in order to account for inaccuracies in Smith's model. All of the computer models, however, basically consist of two components. One component describes the static load-deformation behavior of the soil, and the other component accounts for dynamic effects.

Static Load-Deformation Behavior Models

Static load tests are the best indication of static load-deformation behavior (Fig. 4). Static soil models attempt to accurately depict this behavior, and theoretically, the best soil model available would be the load test itself. For pile driving analysis, however, static load-deformation behavior at the time of driving is required; this behavior may be drastically different from the static load-deformation behavior at the time of the load test.

Lowery et al. (35) developed a generalized soil resistance model (Fig. 5). The model uses the same variables Q(m) and Ru(m) as Smith's curve. The ground quake Q(m) is divided into ten equal pile-soil displacements, and the static soil resistances corresponding to those pile-soil displacements comprise the input data required to establish the curve.

Holloway (26) described a hyperbolic load-deformation model. His

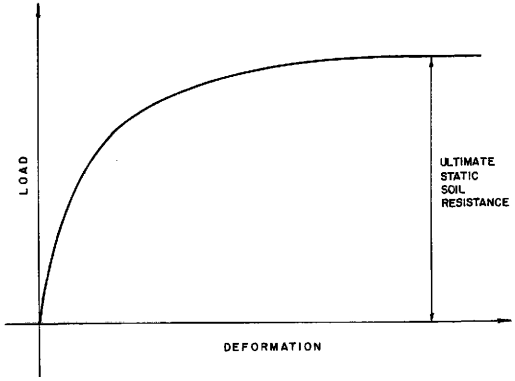

FIG. 4. - Typical Load-Deformation Curve from a Static Load Test

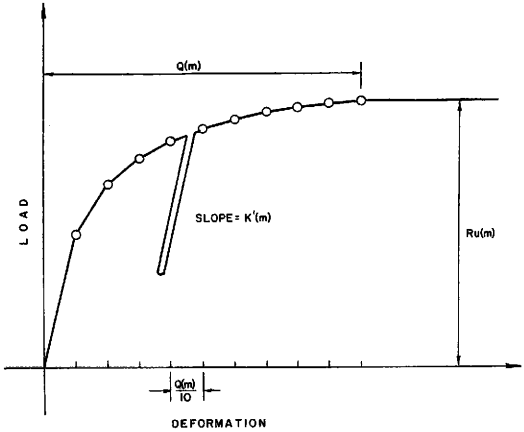

FIG. 5. - Generalized Soil Resistance Model (after Ref. 35)

procedure uses correlation factors to fit a hyperbola to the loading curve of a direct shear test. Two parameters uniquely define a rectangular hyperbola: the initial tangent slope to the curve, and the horizontal asymptote (Fig. 6). For nonlinear tip behavior, Holloway takes the maximum tip load as the asymptote. The initial tangent slope equals the maximum tip load divided by an assumed elastic quake. Holloway recommends a quake value of 0.05 in./ft of pile diameter for piles driven into medium to dense sands. The model assumes linear-elastic unload/reload behavior. The ratio of the unload/reload modulus to the initial tangent modulus is constant for a particular material, but it does not necessarily equal unity.

Bossard and Corte (4) use a bilinear-elastic/plastic load--deformation model. Input requires two slopes K_1 and K_2 plus an unload slope K_3 not necessarily equal to K_1 (Fig. 7). Corresponding ultimate static soil resistances are also required.

E.A.L. Smith's linear-elastic/plastic soil model (43) is the least complicated idealization of static load-deformation behavior. Required input is simply the maximum elastic displacement (quake) and the ultimate static soil resistance (Fig. 8).

The above models attempt to depict static load-deformation behavior of soil during pile driving. One could surmise that the best model would be the generalized model, or perhaps the hyperbolic model, because for sands, they more closely follow the true shape of the static load test curve. The bilinear-elastic/plastic model also closely resembles the static load test curve. Smith's model does not follow the shape as closely as the other models for piles in sands,

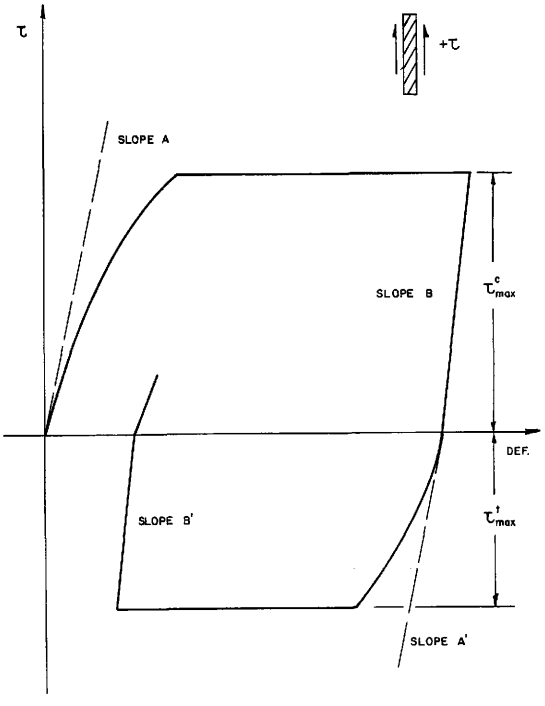

FIG. 6. - Hyperbolic Soil Resistance Model
(after Ref. 26)

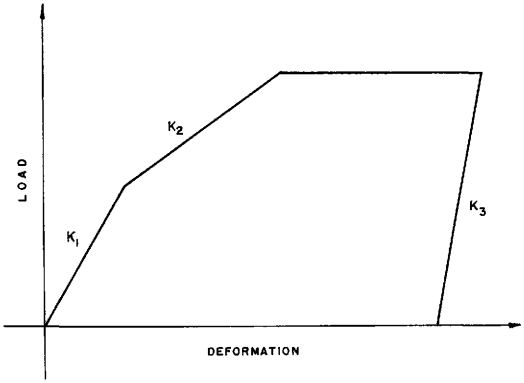

FIG. 7. - Bilinear-Elastic/Plastic Soil Resistance Model (after Ref. 3)

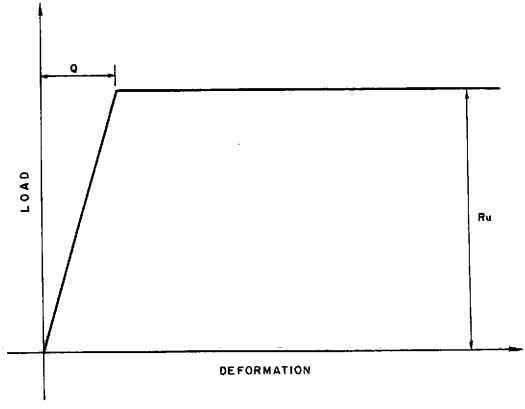

FIG. 8. - Linear-Elastic/Plastic Soil Resistance Model (after Ref. 43)

but its simplicity enhances its attractiveness.

Each model has advantages and disadvantages -- i.e., there is a trade-off between accuracy and simplicity. Lowery (35) compared Smith's model with the generalized model and concluded, "only a drastic change in the soil resistance curve was found to cause an appreciable difference in the solution." Smith's model, then, is a sufficiently accurate depiction of a static load test curve; in other words, its simplicity does not render it invalid.

A legitimate question is, "What is meant by accuracy of the wave equation analysis?" If an engineer uses a wave equation program and determines that driving stresses are not critical in his design, then he has an accurate solution if the pile does not break into pieces during driving. If an engineer uses a wave equation program and determines that a particular hammer will drive a particular pile to a required depth, then he has an accurate solution if the hammer does indeed drive the pile. If an engineer uses a wave equation program to predict bearing capacity, then he has an accurate solution if his predictions correlate well with static load tests.

Correlation with load tests is the most applicable definition of accuracy with respect to soil models. All of the previously mentioned soil models have been correlated with load tests, but Smith's model more than any other. This is by virtue of the fact that it has existed longer than any of the others, and it is the most simple model. The only unknown parameter in Smith's static model, really, is the quake (ultimate resistances are usually chosen to generate a RUT vs. N curve). Not surprisingly, there are different views on the correct value of quake for use in a wave equation computer program.

Quakes

E.A.L. Smith, in this original paper (43), suggested a quake value of 0.1 inches (0.254 cm), " for use until such time as more accurate values become available."[1] In 1965, Forehand and Reese (15) correlated bearing capacity predictions with static load test results by varying quake values from 0.05 in (0.127 cm) to 0.30 in. (0.762 cm). They concluded that Smith's value was acceptable. Lowery et al. (35) varied quake from 0.10 in. (0.254 cm) to 0.50 in. (1.27 cm) with no damping and described the following trend: "The most pronounced and consistent trend is the marked increase in maximum point displacement corresponding to increasing values of Q ... the percent increase in maximum point displacement is relatively small for a small soil resistance, but greatly increases as the total soil resistance becomes large." In their final report, Lowery et al. (34) recommend the value of Q = 0.10 in. (0.254 cm). The quake sensitivity study performed by Ramey and Hudgins (38) is similar to the one by Forehand and Reese, and they arrived at the same conclusions, i.e. Smith's value is acceptable. Roussel (40) also used Smith's quake in his work on large diameter, high capacity, offshore pipe piles. Stevens et al. (46) used Q = 0.1 in. (0.254 cm) when analyzing piles in very dense sand, and rock.

Smith's value, then, has gained widespread acceptance; however, quakes significantly different from his value appear in the literature.

---

[1]The following discussion on quakes makes a distinction between point quakes (Q_{point}) at the pile tip and side quakes (Q_{side}) along the pile shaft. If there is no distinction, Q_{point} equals Q_{side}. Unloading quakes (Q_{unload}) are also discussed. Numerical values are quoted for cohesionless soils.

Coyle et al. (8) determined quake values from static load tests on 16 in. (40.6 cm) *square* concrete piles in sand. They used Q_{point} = 0.4 in. (1.02 cm) and Q_{side} = 0.2 in. (0.51 cm). Authier and Fellenius (1) used dynamic measurements (CAPWAP) and reported quakes on the order of 0.3 in. (0.76 cm) to 0.8 in. (2.03 cm) for two case histories. In the first case history, the soil ws a dense sandy silty glacial till with a 12.8 in. (32.4 cm) closed end pipe pile, and in the second case history, the soil was dense clayey silty glacial till with a 12 in. (30.5 cm) square concrete pile. Thompson (47), commenting on Authier and Fellenius' findings, reported similar high quakes in more coarse grained materials. Likins (32) referenced both Authier and Fellenius and Thompson, and he agreed with them: "The author [Likins] has observed many such "high quake" sands (toe quakes between 0.50 in. (1.27 cm) and 1.0 in. (2.54 cm)) in a wide variety of soil conditions."

Holloway (28) recommends that quake should be proportioned to the effective point diameter for larger diameter displacement piles, e.g., 0.1 in./ft (0.833 cm/m) of diameter. This criterion assumes that the deformation required to fully mobilize tip resistance increases with increasing diameter. These proportionally larger quakes are being used for wave equation analyses of large offshore pipe piles. Table 1 summarizes quake values reported in the literature.

Large quakes significantly affect wave equation results. Authier and Fellenius (1) state: "Where large quakes occur, a given hammer will not be able to drive a given pile to the capacity possible where the ordinary small quake occurs." In other words, a wave equation analysis will show a smaller ultimate static bearing capacity for a

TABLE 1. - Summary of Quake Values for Cohesionless Soils

Source	Loading Quakes		Unloading Quakes	
	Q_{point} (inches)	Q_{side} (inches)	Q_{point} (inches)	Q_{side} (inches)
Smith (43)	0.1	0.1	0.1	0.1
Forehand & Reese (15)	0.1	0.1	0.1	0.1
Lowery, et al. (34)	0.1	0.1	0.1	0.1
Ramey & Hudgins (38)	0.1	0.1	0.1	0.1
Coyle, et al (8)	0.4	0.2	0.1	0.1
Stevens (46)	0.1	0.1	0.1	0.1
Roussel (40)	0.1	0.1	0.1	0.1
Holloway (28)	0.1 in./ft of diameter	not available	not available	not available

Note: 1 in. = 2.54 cm

large quake soil than for a small quake soil, all other things held constant. Thompson (47) does not necessarily believe the large quakes are indicative of the static properties of the soil:

> "This [large] quake does not, however, represent the static properties of the soil. Consequently, in this situation, the Case Method and CAPWAP wave equation analyses would be expected to underpredict bearing capacities. Other wave equation analyses, such as WEAP, would give better predictions if small quakes are employed because they are more representative of static conditions. Ironically, in this case, knowledge of the actual quakes can be detrimental to bearing capacity predictions."

Large quakes in wave equation analyses can cause problems. Coyle et al. (8), using their large quakes determined from static load tests, could achieve no permanent set because the soil never failed plastically during the simulated blow. Fig. 9 illustrates this point. If the assumed RUT equals RUT_2 and if the hammer stress wave deforms the soil only to point G, the soil rebounds along line GO back to point O with no resulting permanent set.

To rectify this situation, Coyle chose an unloading quake less than the loading quake. If Q_{unload} is less than Q_{load}, some amount of permanent set is always obtained. When the assumed RUT is less than the capability of the hammer stress wave (OAB in Fig. 9(a)), the hammer stress wave causes plastic failure in the soil. When the assumed RUT is greater than the capability of the hammer stress wave, the soil does not fail plastically, but there is some permanent set. In Fig. 9(b), when the assumed RUT is RUT_4, the hammer stress wave displaces the soil to point G. Unloading, the soil does not rebound along the loading path GO, but instead rebounds along GH to point H. The resultant permanent set is OH. In this case, the hammer stress

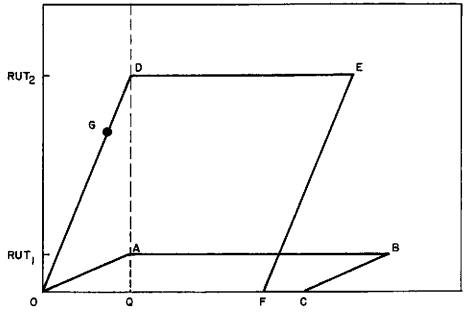

(a) Q-LOADING = Q-UNLOADING

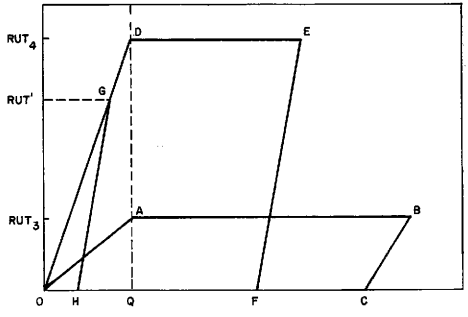

(b) Q-LOADING > Q-UNLOADING

FIG. 9. - Soil Loading Versus Deformation Curves (From Ref. 8)

wave does not overcome the assumed value for RUT_4 but only a fraction of it. To obtain a meaningful bearing graph, the computed blow count must be plotted versus the amount of soil resistance overcome, i.e. RUT'.

Introducing different unloading and loading quakes complicates the soil model - particularly when performing sensitivity studies; there are two more unknown variables. Coyle et al. (8) justified their different unloading quakes on the basis of a previous laboratory research investigation by Dunlap (14) and by field measurements. Stress versus strain data from Dunlap's work indicates that the unloading quake for the soil surrounding a pile may be constant though not necessarily equal to the loading quake. As to the field measurements, the researchers determined the total elastic rebound of the soil by recording gross settlement at full load and at no load and then taking the difference. The unload soil quake is the difference between the elastic rebound and the elastic compression of the pile. From their data, the unloading quake was chosen to be 0.1 in. (0.254 cm). This value proved acceptable for their purpose. Cyclic load tests are the only true way to determine unloading quake values for wave equation analyses.

In summary, static load-deformation models in wave equation computer programs attempt to simulate static load test behavior. The degree of complexity of the models vary. E.A.L. Smith's linear elastic-plastic model, although very simple, is valid and has been correlated with static load tests. Opinions on the proper value of quake for Smith's model vary; a quake value of 0.1 in. (0.254 cm) has wide usage and acceptance, however. The best way to determine quake,

both loading and unloading, is from static or cyclic static load tests. Static load-deformation models only account for static soil behavior; the entire soil model contains both the static component and a dynamic component to account for dynamic driving effects.

Dynamic Soil Behavior Models

Wave equation computer programs use the dynamic soil resistance model in conjunction with the static soil resistance model to determine total driving resistance; total resistance is the sum of the two components. The dynamic component accounts for the fact that soil will offer more instantaneous resistance to rapid motion than to slow motion. The expression for total resistance, in equation form, is:

$$R = S + D \tag{13}$$

where

R = total resistance, F, where F = force

S = static resistance, F

D = dynamic resistance, F

More specifically, the static resistance for an elastic-plastic model (i.e. Smith's) is:

$$S = k_s \cdot d \qquad \text{for } d < q \tag{14a}$$

$$S = S_u \qquad \text{for } d \geq q \tag{14b}$$

where

k_s = soil stiffness, F/L, where L = length

d = pile displacement, L

q = quake, L

S_u = ultimate static resistance, F

The dynamic resistance, in a basic form, is:

$$D = J_v \cdot v \tag{15}$$

where

J_v = viscous damping parameter, $\frac{FT}{L}$ where T = time

v = pile element velocity, L/T.

While J_v is a viscous damping factor, the usual approach in pile driving is to use Smith's original method:

$$D = J \cdot v \cdot S \tag{16}$$

where

J = Smith's damping factor, T/L.

Thus,

$$J = \frac{J_v}{S} \tag{17}$$

The researchers at Case Western Reserve University developed a different form of damping (19) which reflects the average properties

of an element.

$$D = J_c \cdot \frac{EA}{C} \cdot v \tag{18}$$

where

J_c = Case damping factor (dimensionless)

E = Young's modulus for pile element, F/L^2

A = cross-sectional area for pile element, L^2

C = wave speed in pile element, L/T

$\frac{EA}{C}$ = pile impedance, FT/L

In terms of Smith damping, Case damping is:

$$J_c = \frac{J \cdot S}{\frac{EA}{C}} \tag{19}$$

Authier and Fellenius (2) discuss damping parameters, particularly Case damping, in more detail.

Researchers also studied the velocity term in the general dynamic resistance formula. Coyle and Gibson (10, 16) determined that the velocity term should be raised to some power N less than one in order to keep J constant. They studied a range of velocities from 0 ft/sec to 12 ft/sec (3.66 m/sec) and, for a clean sand, they determined the optimum power of N to be 0.20. Heerema (21) agreed with Coyle and Gibson's work for determination of point damping values in wet sand, i.e. the fifth root of velocity relationship. Heerema also noted that point resistance appears very strongly velocity dependent at low velocities, and little velocity dependent at high velocities. Even though the nonlinear relationship is present, Smith's damping values are still in common use.

Smith Damping

Wave equation input parameters, particularly the damping parameters, are the focal point of most criticism of the wave equation method. Dover et al. (13) state:

> "The major existing problem [with the wave equation method] is the bias and uncertainty of the input parameters. This point is highlighted by the common criticism of the wave equation method - one can juggle input parameters and obtain the desired solution. In many cases, this criticism is valid."

Ian Smith (45) states:

> "The major difficulty [with the one-dimensional wave equation] attaches to the estimate of the viscous component of resistance (Smith's parameter, J)."

Holloway et al. (28) adds:

> "Damping parameters described in practice are correlation coefficients, not soil properties. It is quite likely that these damping parameters have masked many unknown inaccuracies in the available case histories."

The preceding statements are not made as an attempt to undermine the credibility of wave equation results; rather, they should help explain the wide range of damping values published in the literature. Roussel (40), commenting on the wide variation of values for damping parameters, states:

> "Notwithstanding these variations, various types of soils have damping parameters that can be placed

between certain bounds."

The following values for Smith damping, as reported in the literature, are for cohesionless soils.

Smith's (43) original damping values are: point damping (Jp) equal 0.15 sec/ft (0.492 sec/m) and side damping (Js) equal 0.05 sec/ft (0.164 sec/m). Holloway et al. (28) reported that CRWU researchers typically reduced the damping parameters toward zero in order to accurately simulate the impact stress wave in a wave equation solution. On the other hand, Goble and Rausche (18) reported a damping value of 2.0 sec/ft (6.56 sec/m) from a CAPWAP analysis. In another report, Goble et al. (17) pointed out a strong tendency for soil damping resistance to be concentrated near the pile tip. Heerema (22) showed that the friction force in sands is not velocity dependent, and that sand behaves as a simple Coulomb material. This implies that Js = 0.0. F.L. Beringen at Fugro B.V. (personal communication, July, 1983) uses Js = 0.0 and Jp = 0.076 sec/ft (0.25 sec/m). Roussel (40) recommends Js = 0.08 sec/ft (0.26 sec/m) and Jp = 0.15 sec/ft (0.492 sec/m). Ramey and Hudgins (38) performed a sensitivity study and recommend Jp = 0.2 - 0.3 sec/ft (0.66 - 0.98 sec/m) and Js = 0.067 - 0.1 sec/ft (0.22 - 0.33 sec/m). Lowery et al. (35) also performed a sensitivity study and noted that as J increases, the maximum pile tip displacement decreases rapidly. They verified Smith's damping values. Table 2 summarizes damping parameter values for cohesionless soils, as reported in the literature.

Summary

The literature review describes recent developments in wave

TABLE 2. - Summary of Smith Damping Values for Cohesionless Soils

Source	Point Damping (sec/ft)	Side Damping (sec/ft)
Smith (43)	0.15	0.05
Heerema (22)	not available	0
Beringen (personal comm.)	0.076	0
Roussel (40)	0.15	0.08
Ramey & Hudgins (38)	0.2 - 0.3	0.067 - 0.10
Lowery, et al. (34)	0.15	0.05

Note: 1 ft = 0.305 m

equation technology, such as the latest applications of wave equation computer analyses. It provides a description of the phenomenon of residual stresses and a brief discussion of dynamic field measurements. The literature review also presents a comprehensive study of computer soil models and the soil input parameters, quake and damping, for cohesionless soils. The in-depth study of soil models and soil input parameters should provide background information for the following sections of this report; i.e., the actual wave equation analysis.

CHAPTER VI

LOCK & DAM NO. 26: PROJECT DESCRIPTION AND ANALYSIS DATA

Project Description

The existing Lock & Dam No. 26 was designed and built in the 1930's and put into operation in 1938 (49). Lock & Dam No. 26 is strategically situated at the center of the 25,000 mile (40,000 km) inland waterway system of the United States. Traffic between the Upper Mississippi, the Illinois, the Ohio River, and the Lower Mississippi Rivers must pass through Lock & Dam No. 26. The structure is located at Alton, Illinois, about 15 miles (24.2 km) downstream of the Illinois River and about 8 miles (12.9 km) upstream of the Missouri River as shown in Fig. 10.

According to the Corps of Engineers (49), there are two major problems with the existing structure. One is inadequate locking capacity. The other problem is a structural one. To solve these problems, a new structure was designed; it will be located approximately three miles (4.8 km) downstream from the existing structure. Construction of the replacement Lock & Dam No. 26 will be carried out in three phases.

Phase I (currently under construction) consists of site preparation, construction of a cofferdam, and construction of the first 6-1/2 gate bays of the main dam structure (see Fig. 11). Phase II consists of constructing another 1/2 gate bay on the dam and the lock itself. This will require construction of a second cofferdam. Phase III involves construction of a two-gate-bay dam section and a closure structure between the lock and the Illinois shore. The target date for construction completion is January, 1989.

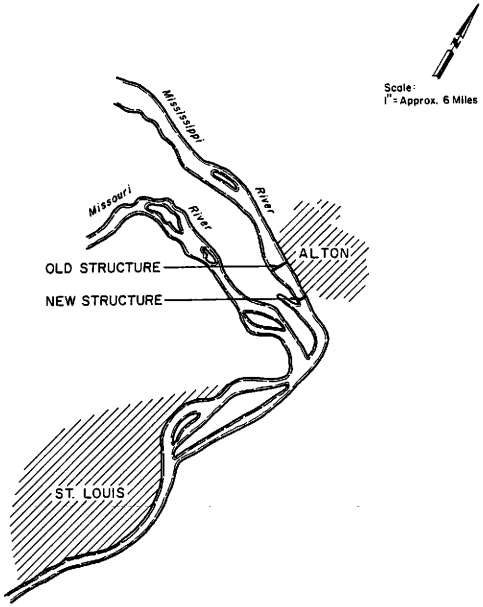

FIG. 10. - Location of the New Lock & Dam No. 26
(From Ref. 49)

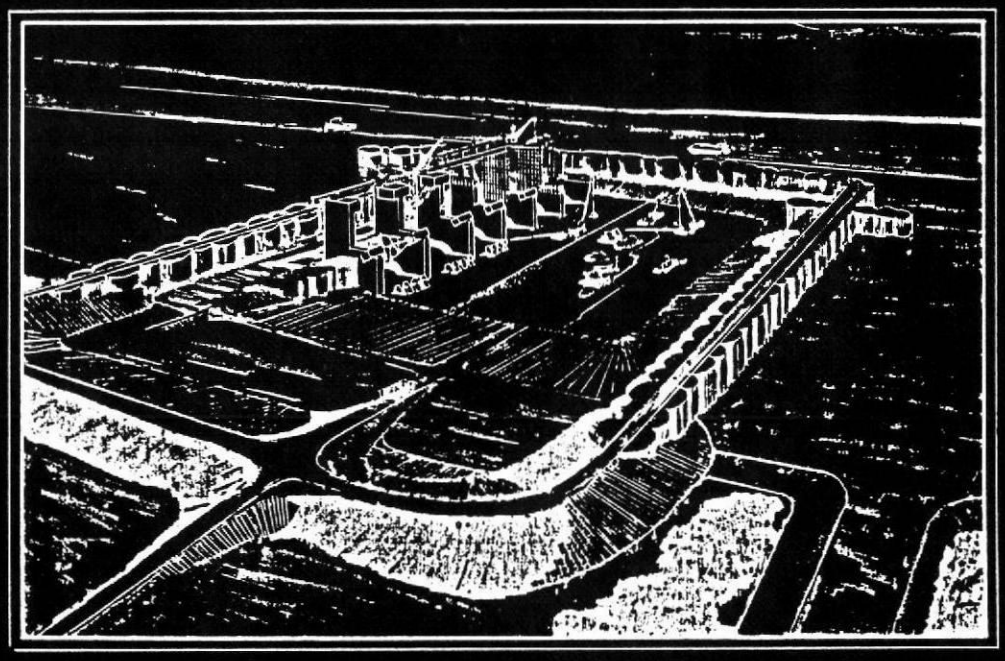

FIG. 11. - Phase I of Construction at Lock & Dam No. 26 (From Ref. 49)

The Test Site

During Phase I construction, test piles were driven in three pile groups as shown in Fig. 12. Fig. 13 and Fig. 14 show the locations of soil borings for Pile Group 1 and Pile Group 2, respectively. Fig. 15 and Fig. 16 show the arrangement of the piles in Pile Group 1 and Pile Group 2, and the locations of the piles which were load tested. Huff (30) provides a more complete description of the test site and of the particular tests performed at each pile group.

Soil Description

The soil consists of fine to medium grained poorly graded sand with fine to coarse gravel and occasional traces of coarse sand. Pebbles and cobbles were present at different depths, as shown in the standard penetration test borings (Fig. 17 through Fig. 20). Fig. 21 shows the gradation band from a sieve analysis test. In Boring B-3 (Fig. 17), pebbles and cobbles were found from 12 ft (3.7 m) depth to the lower boundary of the boring. Pebbles and cobbles were not found in Boring B-21 (Fig. 19). Three of the boring logs show a layer of coarse gravel and cobbles extending from approximately 55.5 ft to 57 ft (17.0 m to 17.4 m). Glacial till consisting of sand and gravel within firm gray/green clay was encountered from 58 ft to 63 ft (17.7 m to 19.3 m); limestone underlaid the glacial till in all borings except B-20 (Fig. 20).

In Situ Tests

Three types of in situ tests were performed at the site. These were the standard penetration test (SPT), the cone penetrometer test (CPT), and the pressuremeter test (PMT).

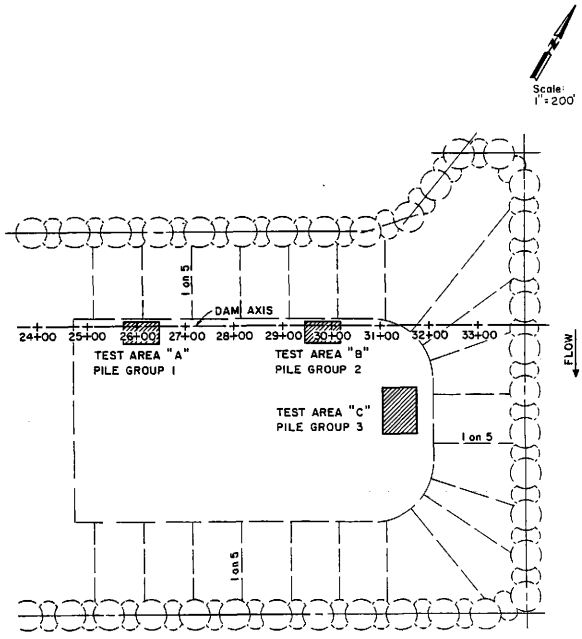

FIG. 12. - Location of Pile Groups During Phase I of Construction (From Ref. 30)

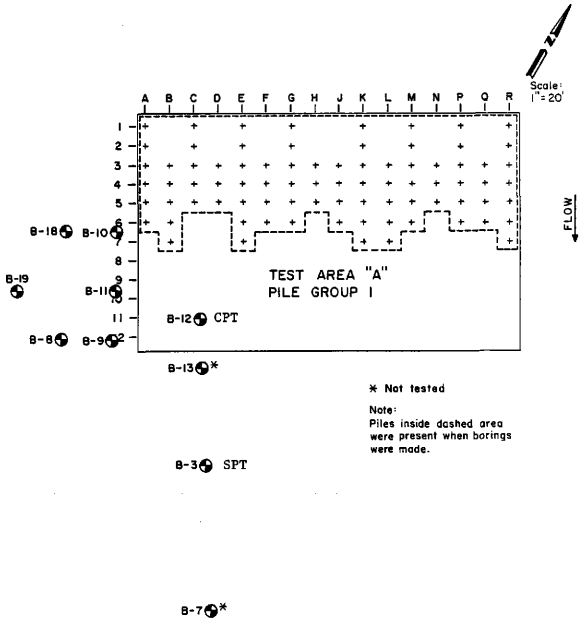

FIG. 13. - In Situ Test Boring Locations for Pile Group 1 (From Ref. 30)

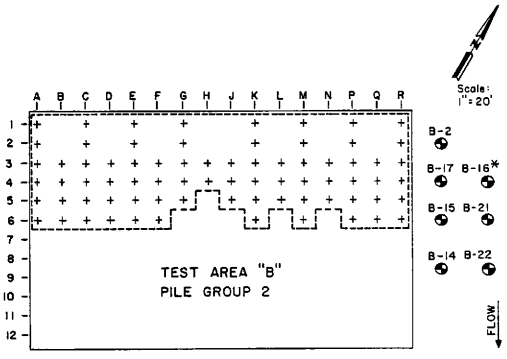

* Not tested

Note:
Piles inside dashed area were present when borings were tested.

FIG. 14. - In Situ Test Boring Locations for Pile Group 2 (From Ref. 30)

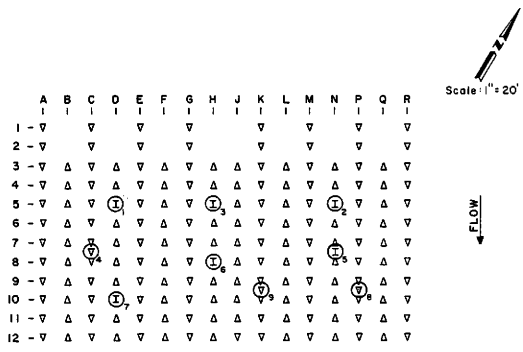

△ BATTERED PILE, ARROW SHOWS DIRECTION OF BATTER

Ⓣ VERTICAL TEST PILE

Ⓐ BATTERED TEST PILE

FIG. 15. - Location of Test Piles in Pile Group 1 (From Ref. 30)

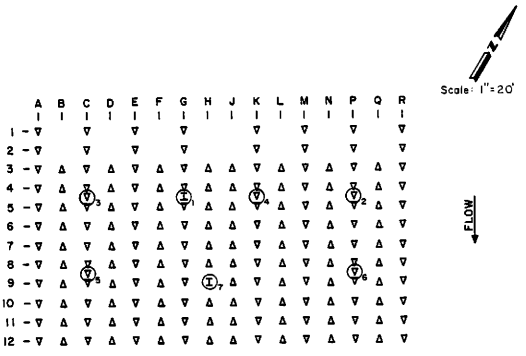

Δ BATTERED PILE, ARROW SHOWS DIRECTION OF BATTER
Ⓘ VERTICAL TEST PILE
Ⓐ BATTERED TEST PILE

FIG. 16. - Location of Test Piles in Pile Group 2
(From Ref. 30)

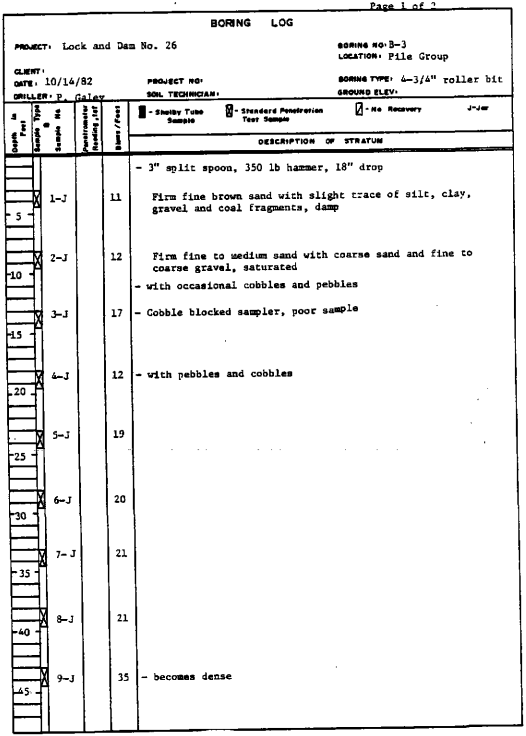

Page 1 of 2

BORING LOG

PROJECT: Lock and Dam No. 26 — BORING NO: B-3 — LOCATION: Pile Group

CLIENT:
DATE: 10/14/82 — PROJECT NO: — BORING TYPE: 4-3/4" roller bit
DRILLER: P. Galey — SOIL TECHNICIAN: — GROUND ELEV:

■ - Shelby Tube Sample ▽ - Standard Penetration Test Sample ☒ - No Recovery J-Jar

Depth In Feet	Sample Type & No.	Penetrometer Reading, tsf	Blows / Foot	DESCRIPTION OF STRATUM
				- 3" split spoon, 350 lb hammer, 18" drop
5	1-J		11	Firm fine brown sand with slight trace of silt, clay, gravel and coal fragments, damp
10	2-J		12	Firm fine to medium sand with coarse sand and fine to coarse gravel, saturated
				- with occasional cobbles and pebbles
15	3-J		17	- Cobble blocked sampler, poor sample
20	4-J		12	- with pebbles and cobbles
25	5-J		19	
30	6-J		20	
35	7-J		21	
40	8-J		21	
45	9-J		35	- becomes dense

FIG. 17. - Soil Boring Log for Boring No. B-3 (From Ref. 30)

BORING LOG

PROJECT: Lock and Dam No. 26 — BORING NO: B-3
LOCATION: Pile Group
CLIENT:
DATE: 10/14/82 — PROJECT NO: — BORING TYPE: 4/3/4" roller bit
DRILLER: — SOIL TECHNICIAN: — GROUND ELEV:

■ - Shelby Tube Sample ☒ - Standard Penetration Test Sample ☑ - No Recovery

Depth in Feet	Sample Type	Sample No.	Penetration Resistance, Blows/Foot	Blows / Foot	DESCRIPTION OF STRATUM
50		10-J		30	
55		11-J		34	
					56'
					Coarse gravel, pebbles and cobbles
					57'
60		12-J		32	Hard gray/green clay with sand and gravel (Glacial till)
					Limestone at 59.5"
					Bottom at 59.5'
65					
70					
75					
80					
85					
90					

FIG. 17. - (Continued)

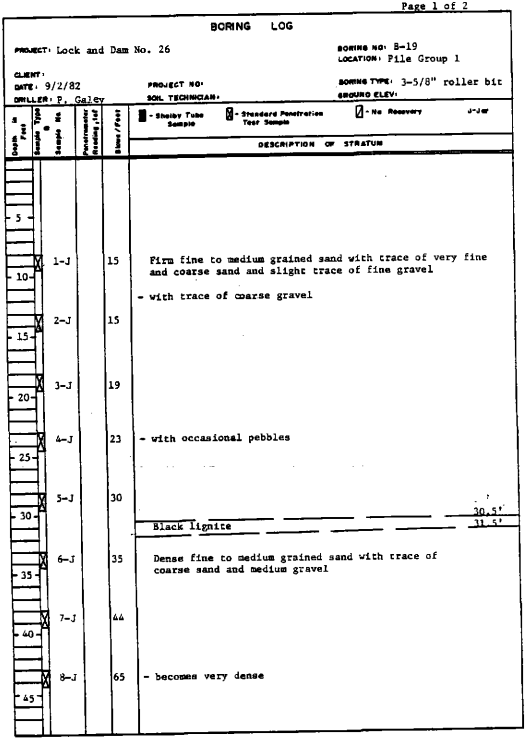

Page 1 of 2

BORING LOG

PROJECT: Lock and Dam No. 26
BORING NO: B-19
LOCATION: Pile Group 1
CLIENT:
DATE: 9/2/82
PROJECT NO:
BORING TYPE: 3-5/8" roller bit
DRILLER: P. Galey
SOIL TECHNICIAN:
GROUND ELEV:

■ - Shelby Tube Sample ⊠ - Standard Penetration Test Sample ⊘ - No Recovery J-Jar

Depth in Feet	Sample Type & Sample No.	Penetrometer Reading, tsf	Blows / Foot	DESCRIPTION OF STRATUM
5				
10	1-J		15	Firm fine to medium grained sand with trace of very fine and coarse sand and slight trace of fine gravel
				- with trace of coarse gravel
15	2-J		15	
20	3-J		19	
	4-J		23	- with occasional pebbles
25				
30	5-J		30	30.5'
				Black lignite 31.5'
35	6-J		35	Dense fine to medium grained sand with trace of coarse sand and medium gravel
	7-J		44	
40				
45	8-J		65	- becomes very dense

FIG. 18. - Soil Boring Log for Boring No. B-19
(From Ref. 30)

BORING LOG

PROJECT: Lock and Dam No. 26 BORING NO: B-19
LOCATION: Pile Group 1
CLIENT:
DATE: 9/2/82 PROJECT NO: BORING TYPE: 3-5/8" roller bit
DRILLER: SOIL TECHNICIAN: GROUND ELEV:

■ - Shelby Tube Sample ▨ - Standard Penetration Test Sample ☑ - No Recovery J-Jar

Depth in Feet	Sample Type & No.	Penetrometer Reading, tsf	Blows / Foot	DESCRIPTION OF STRATUM
50	9-J		54	
55	10-J		66	- cobble at 55.5' - cobble at 57' 57.5'
60				Hard gray/green clay with trace of silt, sand, gravel and wood (Glacial till) Bottom at 59.5'
65				
70				
75				
80				
85				
90				

FIG. 18. - (Continued)

Page 1 of 2

BORING LOG

PROJECT: Lock and Dam No. 26 — BORING NO: B-21 — LOCATION: Pile Group 2

CLIENT:

DATE: 9/27/82 & 9/28/82 — PROJECT NO: — BORING TYPE: 4-3/4" roller bit

DRILLER: P. Galey — SOIL TECHNICIAN: — GROUND ELEV:

■ - Shelby Tube Sample ☒ - Standard Penetration Test Sample ☐ - No Recovery J-Jar

Depth in Feet	Sample Type & Sample No.	Penetration Resisting per 6 inches	Blows / Foot	DESCRIPTION OF STRATUM
				- 3" split spoon sampler, 350 lb hammer, 18" drop
5	1-J		19	Firm gray fine sand with trace of medium sand and fine to medium gravel
10	2-J		21	- with fine to coarse gravel
				- with occasional coarse gravel
15	3-J		17	-
20	4-J		20	Firm very fine to fine dark gray sand with trace of gravel
				- coarse gravel or small cobbles from 21.5' to 22'
25	5-J		14	Firm medium to coarse grained sand with trace of fine to coarse gravel
30	6-J		15	
35	7-J		25	
40	8-J		18	
45	9-J		62	- becomes very dense

FIG. 19. - Soil Boring Log for Boring No. B-21 (From Ref. 30)

BORING LOG

PROJECT: Lock and Dam No. 26 BORING NO: B-21
LOCATION: Pile Group 2
CLIENT:
DATE: 9/27/82 & 9/28/82 PROJECT NO: BORING TYPE: 4-3/4" roller bit
DRILLER: SOIL TECHNICIAN: GROUND ELEV:

■ - Shelby Tube Sample ⊠ - Standard Penetration Test Sample ☑ - No Recovery J-Jar

Depth in Feet	Sample Type & Sample No.	Penetrometer Reading, tsf	Blows / Foot	DESCRIPTION OF STRATUM
50	10-J		27	- becomes firm
55	11-J		59	- becomes very dense
60	12-J		41	- becomes dense
				62.5'
65	13-J		59	Hard clay with gravel and sand (Glacial till) - cobble at 65'
				66'
				Limestone
				Bottom at 67'
70				
75				
80				
85				
90				

FIG. 19. - (Continued)

BORING LOG

PROJECT: Lock and Dam No. 26
BORING NO: B-20
LOCATION: Pile Group 3
CLIENT:
DATE: 9/2/82 and 9/3/82 PROJECT NO:
BORING TYPE: 3-5/8" roller bit
DRILLER: P. Galey
SOIL TECHNICIAN:
GROUND ELEV:

■ - Shelby Tube Sample ▨ - Standard Penetration Test Sample ▯ - No Recovery J-Jar

Depth, Feet	Sample Type	Sample No.	Penetrometer Reading, tsf	Blows/Foot	DESCRIPTION OF STRATUM
					Sand with pea-sized gravel and trace of coarse gravel
5					- coarse gravelly layer from 4.8' to 5.5'
10	▨	1-J		18	Firm fine gray sand with trace of fine gravel
15	▨	2-J		14	- with trace of coarse gravel
20	▨	3-J		36	- becomes dense with more gravel
25	▨	4-J		42	
30	▨	5-J		27	- becomes firm
35	▨	6-J		35	- becomes dense
40	▨	7-J		40	
45	▨	8-J		67	- becomes very dense with trace of pebbles - with occasional large pebbles

FIG. 20. - Soil Boring Log for Boring No. B-20 (From Ref. 30)

BORING LOG

PROJECT: Lock and Dam No. 26 BORING NO: B-20
LOCATION: Pile Group 3
CLIENT:
DATE: 9/2/82 and 9/3/82 PROJECT NO: BORING TYPE: 3-5/8" roller bit
DRILLER: SOIL TECHNICIAN: GROUND ELEV:

Depth in Feet	Sample Type & Sample No.	Penetrometer Reading, tsf	Blows / Foot	■ - Shelby Tube Sample ☒ - Standard Penetration Test Sample ☑ - No Recovery J-Jar DESCRIPTION OF STRATUM
50	☒ 9-J		34	- becomes dense
				- cobbles from 52.8' to 53.2'
55	☒ 10-J		47	
				- cobbles from 56.5' to 57.2'
60	☒ 11-J		66	
				Bottom at 59.5'
65				
70				
75				
80				
85				
90				

FIG. 20. - (Continued)

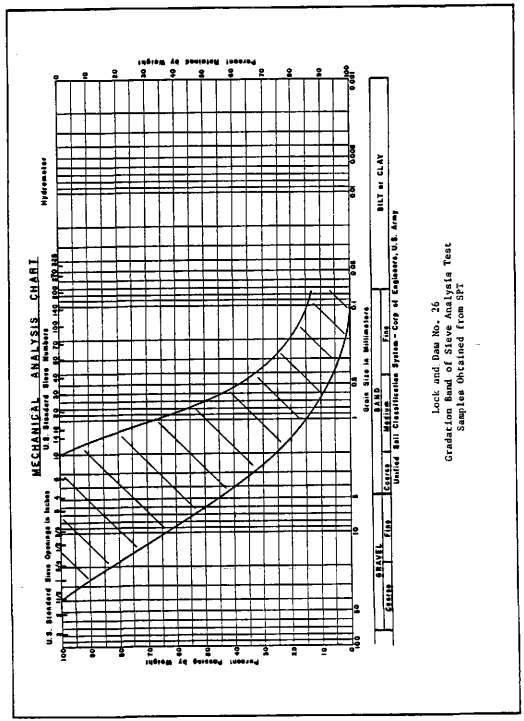

Lock and Dam No. 26
Gradation Band of Sieve Analysis Test
Samples Obtained from SPT

FIG. 21. - Gradation Band of Sieve Analysis Test
(From Ref. 30)

Fig. 22 shows the SPT results. At a depth of 55 ft (17 m) the penetration resistance varies from 45 blows/ft to 80 blows/ft (147 blows/m to 262 blows/m).

Fig. 23 and Fig. 24 apply to the CPT. At 55 ft (17 m) depth, the tip resistance is approximately 2020 psf (200 kg/cm^2).

Fig. 25 through Fig. 30 provide PMT information. Fig. 25 and Fig. 28 show an average net limit pressure of approximately 460 psi (3200 kPa) at 55 ft (17 m) depth. Fig. 26 and Fig. 29 show an average initial pressuremeter modulus of 5070 psi (35,000 kPa), and Fig. 27 and Fig. 30 show an average reload modulus of approximately 16,700 psi (115,000 kPa). Huff (30) describes the in situ testing, particularly the pressuremeter test, in detail.

Pile Load Test Data

The Corps of Engineers authorized 34 instrumented pile load tests at the Lock & Dam No. 26 site: 10 tests in Pile Group 1, 8 tests in Pile Group 2, and 16 tests in Pile Group 3. The piles were instrumented with "telltales" which measure axial deflection at various depths along the pile. Table 3 lists the test piles, the types of load test, and pertinent pile data. The Corps of Engineers provided the following information from each pile load test:

(a) Plot of Pilehead Movement and Piletip Movement vs. Applied Load.

(b) Driving Record

(c) Axial Deflection and Load Distribution vs. Pile Depth Curves with Associated Tables

Exceptions to the above data are as follows:

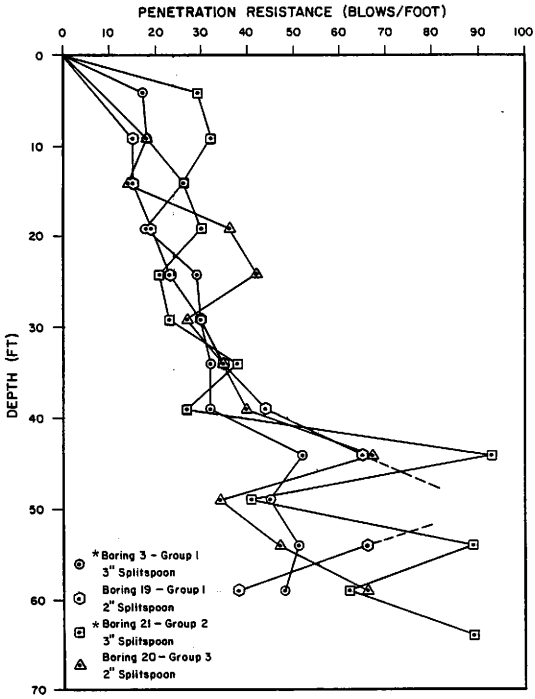

* NOTE: Penetration Resistance Shown has been multiplied by 1.5

FIG. 22. - Standard Penetration Test Results Obtained from Borings at Lock & Dam No. 26 (1 ft = .305 m) (From Ref. 30)

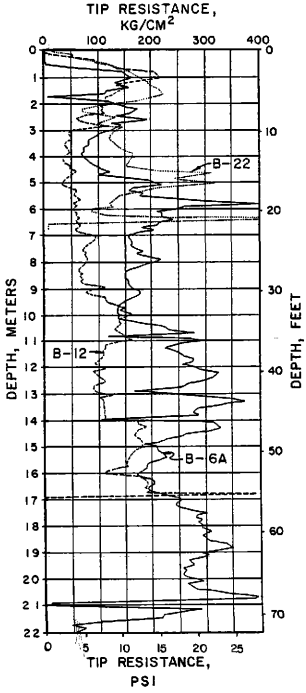

FIG. 23. - Cone Penetrometer Data: Tip Resistance Versus Depth (1 kg/cm^2 = 0.0703 psi, 1 m = 3.28 ft)(From Ref. 30)

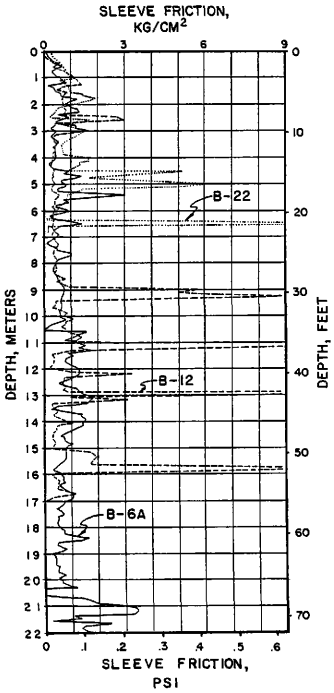

FIG. 24. - Cone Penetrometer Data: Sleeve Friction Versus Depth ($1\ kg/cm^2 = 0.0703$ psi, $1\ m = 3.28$ ft)(From Ref. 30)

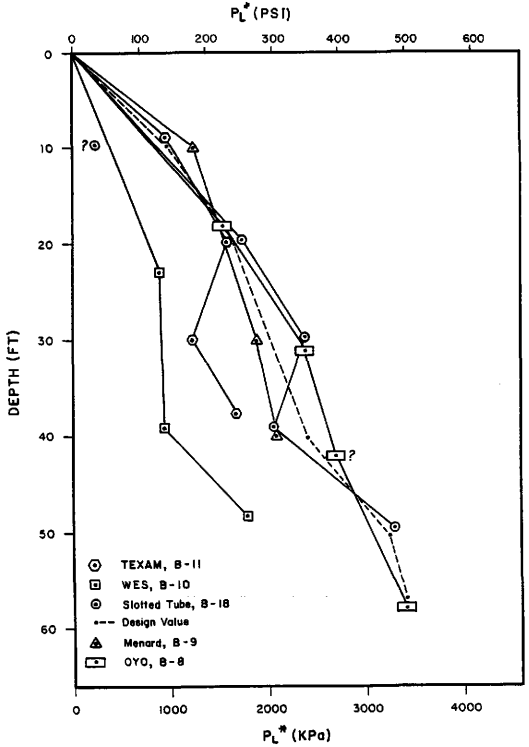

FIG. 25. - Pressuremeter Data: Net Limit Pressure Versus Depth for Pile Group 1 (1 kPa = 0.145 psi, 1 ft = .305 m) (From Ref. 30)

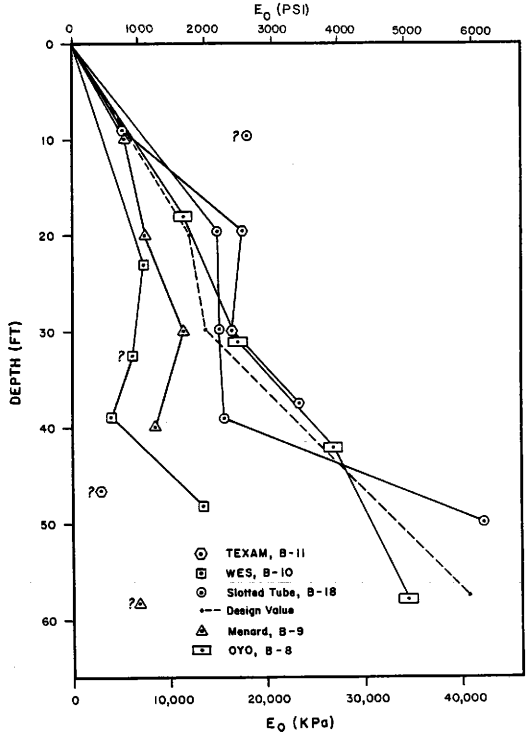

FIG. 26. - Initial Pressuremeter Modulus Versus Depth for Pile Group 1 (1 kPa = 0.145 psi, 1 ft = .305 m)(From Ref. 30)

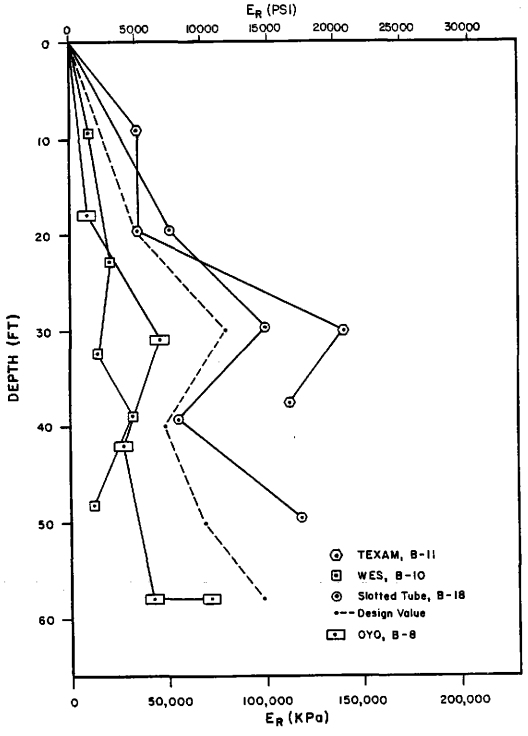

FIG. 27. - Reload Pressuremeter Modulus Versus Depth for Pile Group 1 (1 kPa = 0.145 psi, 1 ft = .305 m)(From Ref. 30)

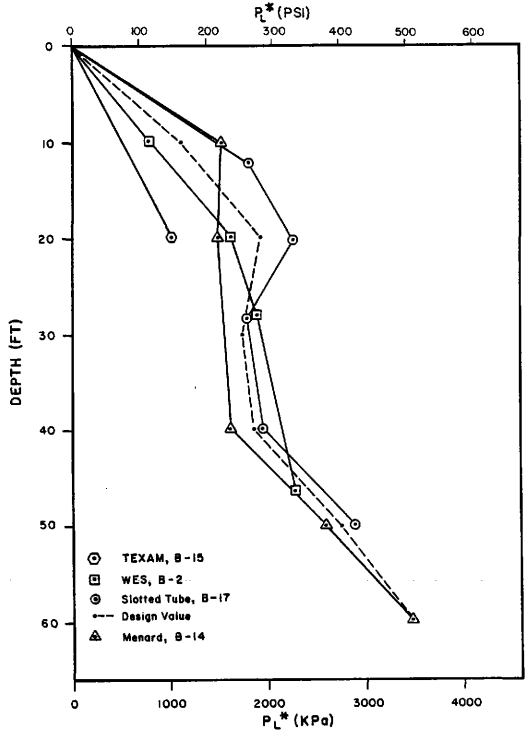

FIG. 28. ~ Pressuremeter Data: Net Limit Pressure Versus Depth for Pile Group 2 (1 kPa = 0.145 psi, 1 ft = .305 m) (From Ref. 30)

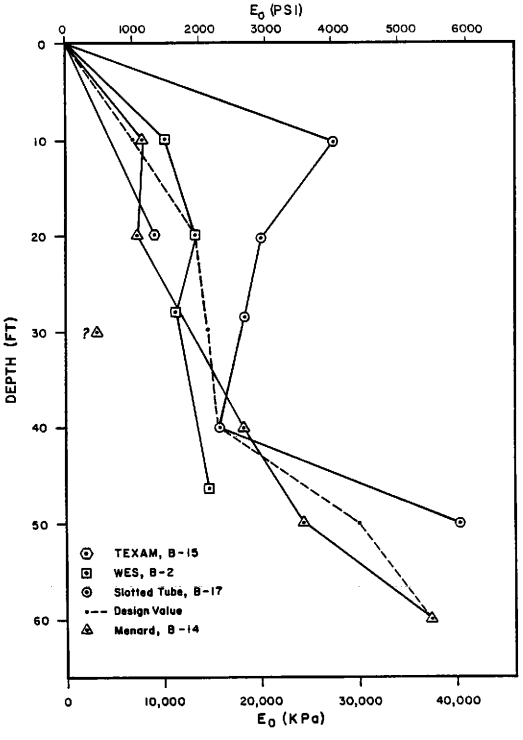

FIG. 29. - Initial Pressuremeter Modulus Versus Depth for Pile Group 2 (1 kPa = 0.145 psi, 1 ft = .305 m)(From Ref. 30)

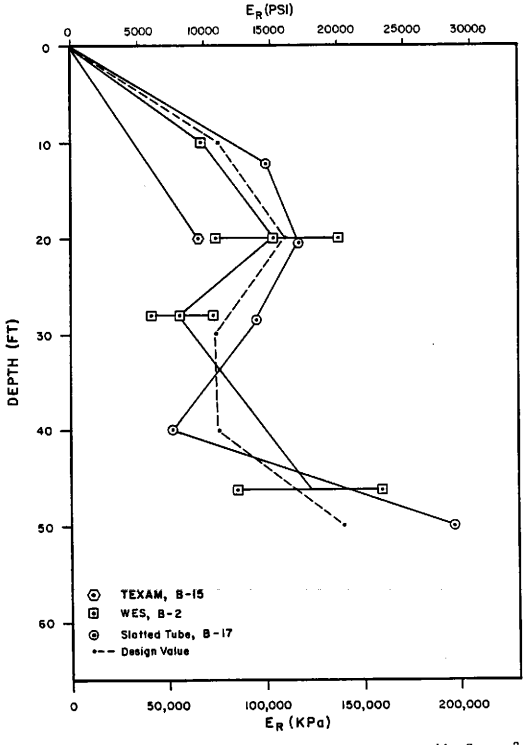

FIG. 30. - Reload Pressuremeter Modulus Versus Depth for Pile Group 2 (1 kPa = 0.145 psi, 1 ft = .305 m)(From Ref. 30)

TABLE 3. - Lock & Dam No. 26 Pile Load Test Summary

DESCRIPTION OF PILE									
Pile	Date Driven	Begin Load Test	Test Type	Type Pile	Axial Pile Length	Batter	Vertical Projected Length	Surface Elevation	Tip Elevation
1-1	8/14/82	8/18/82	Long Vertical ASTM Tens.	HP14x73	60.75	Vert	60.75	359.00	298.25
1-2	8/25/82	8/29/82	Short Vertical ASTM Tens.	HP14x73	54.00	Vert	54.00	357.70	303.70
1-3A	8/26/82	9/2/82	Short Vertical ASTM Comp.	HP14x73	54.00	Vert	54.00	357.70	303.70
1-3B	8/26/82	9/5/82	Short Vertical ASTM Tens.	HP14x73	54.00	Vert	54.00	357.70	303.70
1-4	9/10/82	9/14/82	Long Batter ASTM Tens.	HP14x73	65.00	1:2.5	60.35	357.40	297.05
1-5	9/10/82	9/18/82	Long Vertical Quick Tens.	HP14x73	60.50	Vert	60.50	357.70	296.50
1-6	10/7/82	10/18/82	Short Vertical Quick Comp.	HP14x73	53.00	Vert	53.00	357.40	304.40
1-7	9/24/82	10/4/82	Long Vertical Quick Comp.	HP14x73	59.00	Vert	59.00	357.60	298.60
1-8	9/22/82	9/27/82	Long Batter Quick Comp.	HP14x73	66.00	1:2.5	61.23	357.40	296.12
1-9	9/23/82	9/30/82	Short Batter Quick Comp.	HP14x73	58.00	1:2.5	53.85	357.60	303.75
2-1	8/25/82	8/30/82	Short Vertical Quick Tens.	HP14x73	55.00	Vert	55.00	357.30	302.30
2-2	8/18/82	8/24/82	Short Batter Quick Tens.	HP14x73	59.00	1:2.5	55.00	359.00	304.00
2-3	8/27/82	9/3/82	Long Batter Quick Tens.	HP14x73	69.20	1:2.5	64.25	358.70	294.45
2-4	8/26/82	8/31/82	Short Batter ASTM Tens.	HP14x73	58.00	1:2.5	53.85	359.00	305.15
2-5	9/28/82	10/6/82	Short Batter ASTM Comp.	HP14x73	59.00	1:2.5	54.78	358.60	308.82
2-6	9/13/82	9/23/82	Long Batter ASTM Comp.	HP14x73	71.17	1:2.5	66.08	357.70	296.12
2-7	9/16/82	9/29/82	Long Vertical ASTM Comp.	HP14x73	66.83	Vert	66.83	358.50	291.67
2-8	10/29/82	11/3/82	Short Vertical ASTM Tens.	HP14x73	40.00	Vert	40.00	359.00	319.00
3-1	12/1/82	12/28/82	Short Vertical ASTM Comp.	12"OD Pipe	46.70	Vert	46.70	360.70	314.00
3-2	12/1/82	1/4/83	Short Vertical ASTM Tens.	12"OD Pipe	36.00	Vert	36.00	360.00	324.00
3-3			NOT USED						
3-4	12/1/82	1/3/83	Short Vertical ASTM Comp.	14"OD Pipe	47.20	Vert	47.20	361.2	314.00
3-5	12/1/82	12/28/82	Short Vertical ASTM Tens.	14"OD Pipe	36.50	Vert	36.50	360.5	324.00
3-6			NOT USED						
3-7	12/1/82	1/7/83	Short Vertical ASTM Comp.	16"OD Pipe	47.80	Vert	47.80	361.80	314.00
3-8	12/1/82	12/29/82	Short Vertical ASTM Tens.	16"OD Pipe	36.50	Vert	36.50	360.50	324.00
3-9			NOT USED						
3-10	12/28/82	1/6/83	Long Vertical ASTM Comp.	HP14x117	65.67	Vert	65.67	355.00	289.33
3-11			NOT USED						
3-12			Lateral Load Test						
3-13			Lateral Load Test						
3-14	11/18/82	3/14/83	Short Vertical Quick Tens.	HP14x73	39.00	Vert	39.00	364.00	325.00
3-15	11/10/82	3/23/83	Short Vertical Quick Tens.	HP14x73	37.00	Vert	37.00	359.00	322.00
3-16	3/25/82	4/27/83	Short Vertical Quick Tens.	HP14x73	37.00	Vert	37.00	364.00	327.00

Note: 1 ft = .305 m

(a) No driving record was available for Pile Load Test 8, Group 2.

(b) Axial Deflection and Load Distribution curves were not available for Pile Load Test 4, Group 2 and Piles 1, 4, and 7 in Group 3.

(c) Only pilehead deflections and tip deflections were measured on Test Pile 8, Group 2 and Test Piles 14, 15, and 16, Group 3.

The primary analysis objective is to determine soil input parameters for the wave equation computer program. The analysis method (described in the next chapter) uses the load test data, and certain requirements are necessary for a load test to be applicable to the analysis. The requirements are:

(a) The test must be a compression test.

(b) The test must be to failure, i.e. the pile must plunge.

(c) Driving records, axial deflection curves, and load distribution curves must be available.

Only four pile load tests met or came close to meeting the above criteria. They are the tests on Pile 1-3A, Pile 1-6, Pile 1-9, and Pile 2-5. All of these piles are HP 14 x 73 shapes.

Fig. 31 through Fig. 34 are the Load vs. Pilehead Movement curves; these curves were used to determine ultimate static soil resistance. Fig. 35 through Fig. 38 are the Point Load vs. Point Deflection curves, and Fig. 39 through Fig. 42 are the Friction Load vs. Average Deflection curves for the four piles. These curves were obtained from the given Axial Deflection curves and Load Distribution curves; they

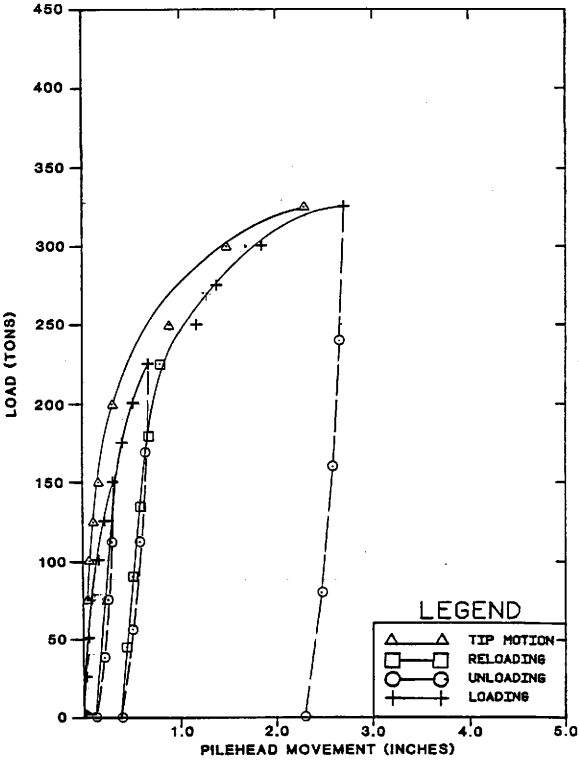

FIG. 31. - Load Versus Pilehead Movement for Pile 1-3A

(1 ton = 8.896 kN; 1 in. = 2.54 cm)

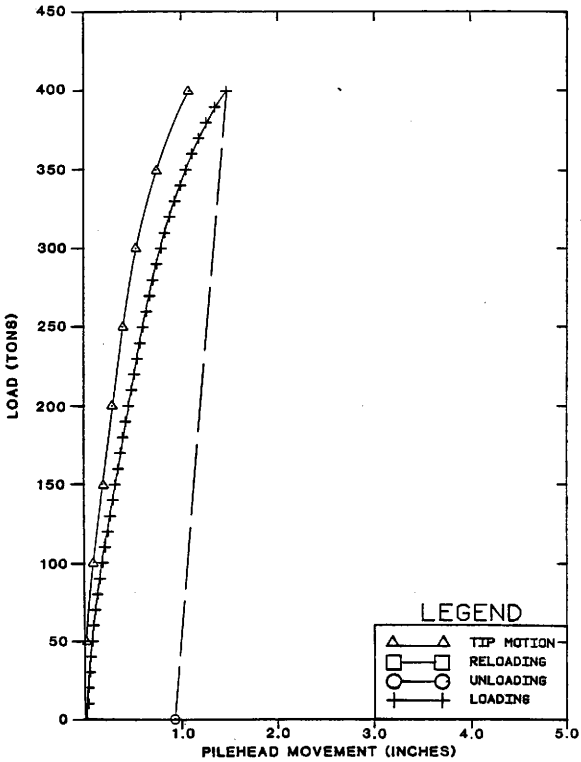

FIG. 32. - Load Versus Pilehead Movement for Pile 1-6

(1 ton = 8.896 kN; 1 in. = 2.54 cm)

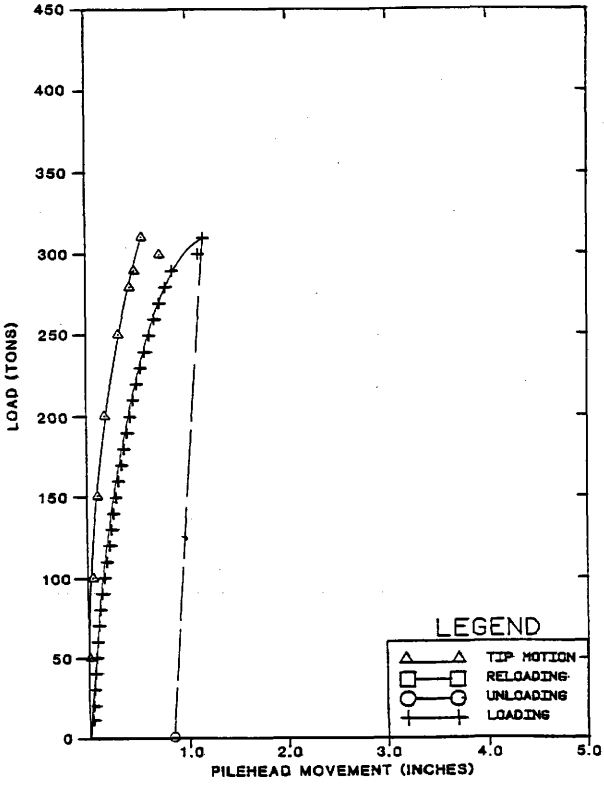

FIG. 33. - Load Versus Pilehead Movement for Pile 1-9

(1 ton = 8.896 kN; 1 in. = 2.54 cm)

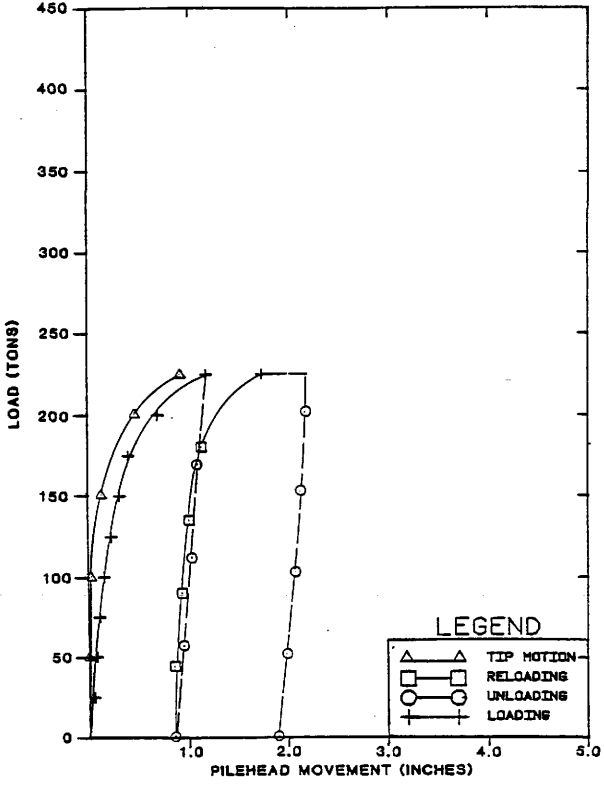

FIG. 34. - Load Versus Pilehead Movement for Pile 2-5

(1 ton = 8.896 kN; 1 in. = 2.54 cm)

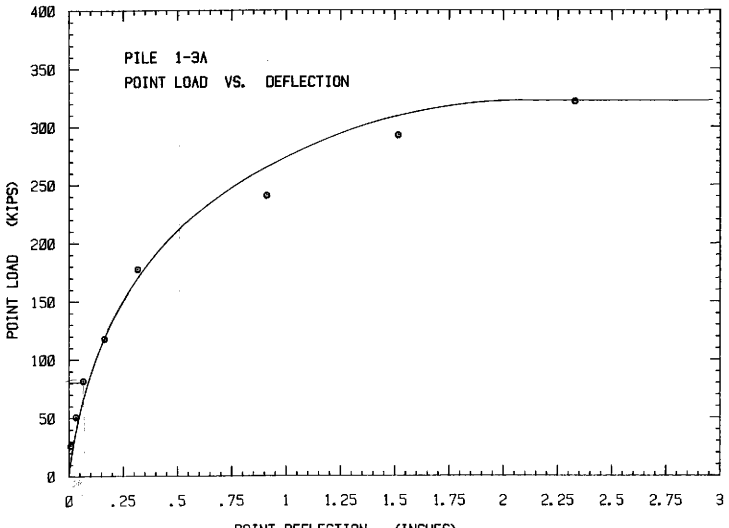

FIG. 35 - Point Load Versus Point Deflection for Pile 1-3A (1 kip = 4.448 kN; 1 in. = 2.54 cm)

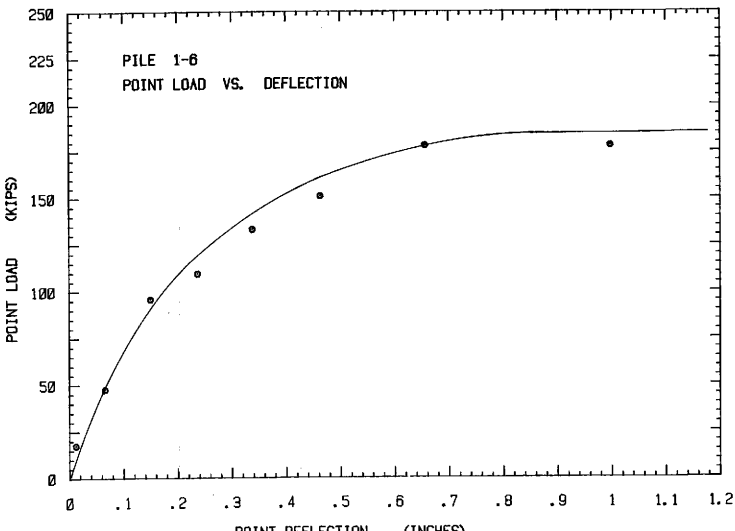

FIG. 36 - Point Load Versus Point Deflection for Pile 1-6 (1 kip = 4.448 kN; 1 in. = 2.54 cm)

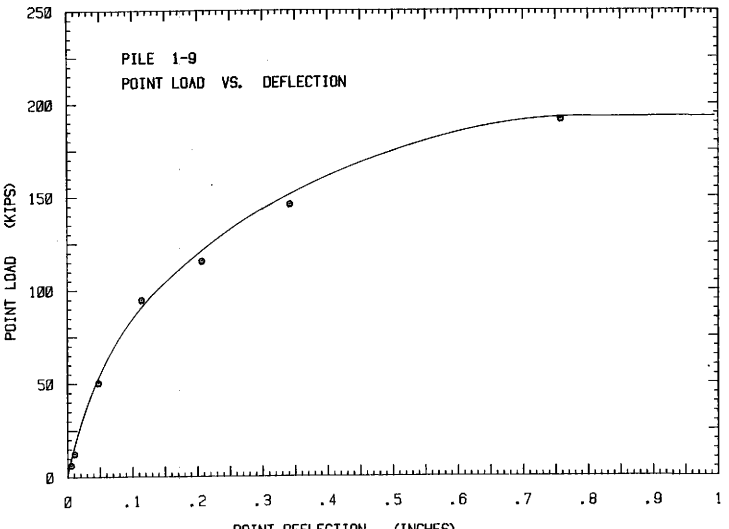

FIG. 37 - Point Load Versus Point Deflection for Pile 1-9 (1 kip = 4.448 kN; 1 in. = 2.54 cm)

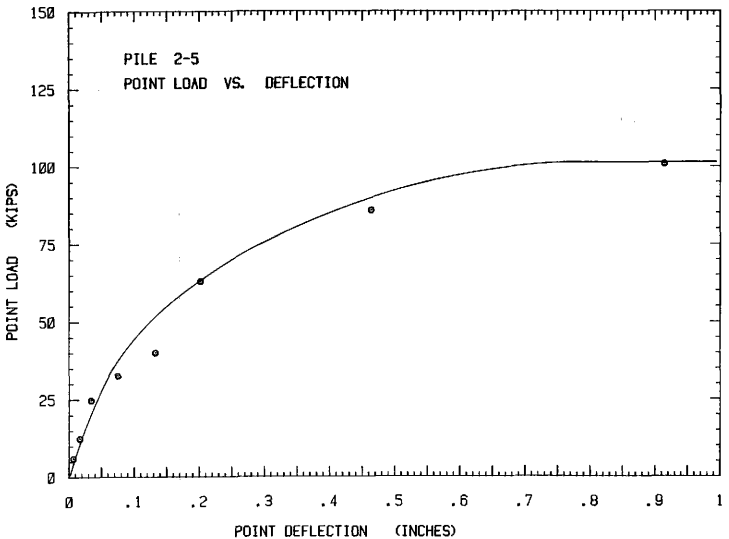

FIG. 38 - Point Load Versus Point Deflection for Pile 2-5 (1 kip = 4.448 kN; 1 in. = 2.54 cm)

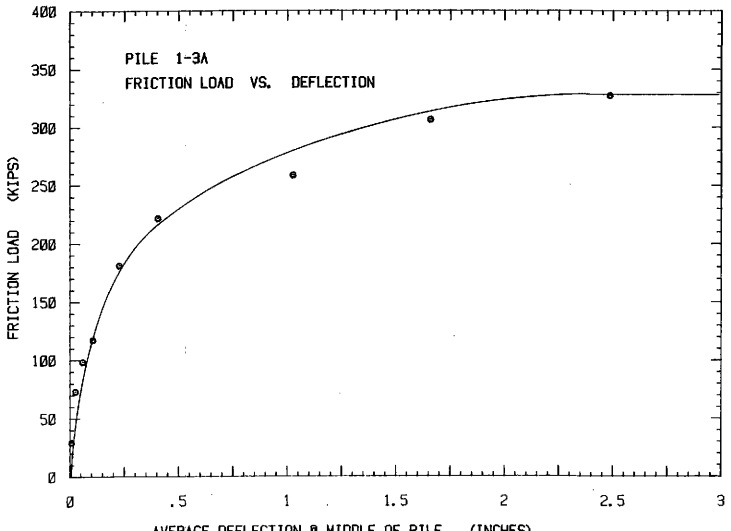

FIG. 39 - Friction Load Versus Average Deflection for Pile 1-3A (1 kip = 4.448 kN; 1 in. = 2.54 cm)

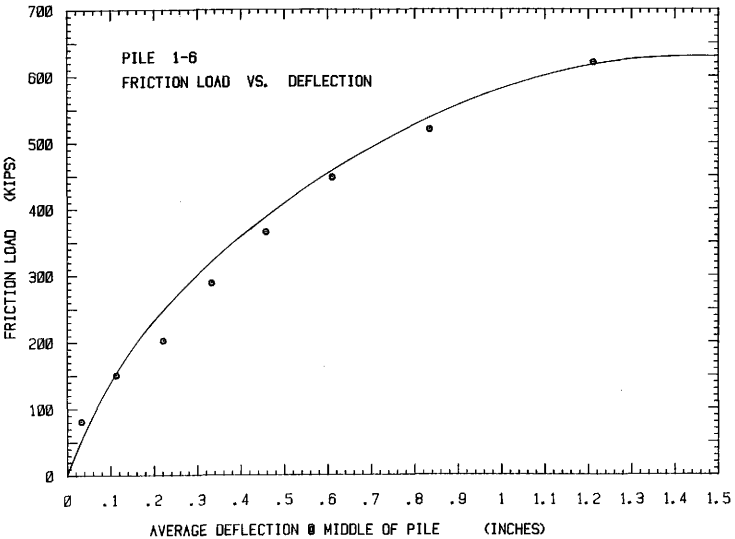

FIG. 40 - Friction Load Versus Average Deflection for Pile 1-6 (1 kip = 4.448 kN; 1 in. = 2.54 cm)

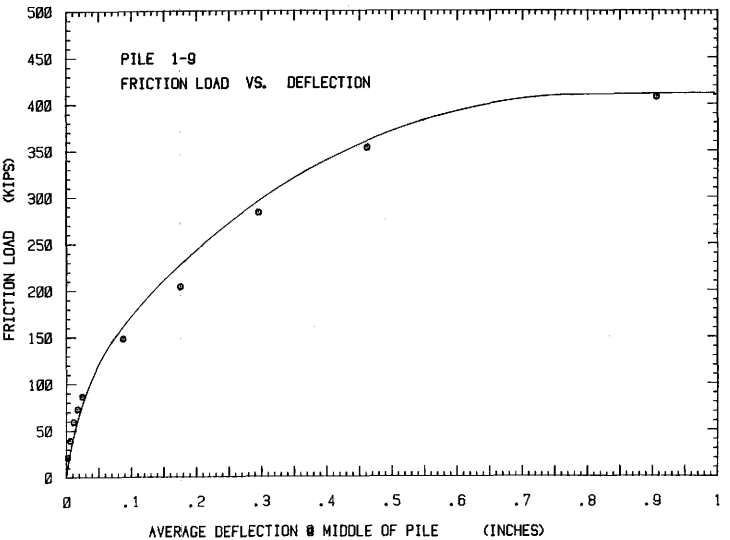

FIG. 41 - Friction Load Versus Average Deflection for Pile 1-9 (1 kip = 4.448 kN; 1 in. = 2.54 cm)

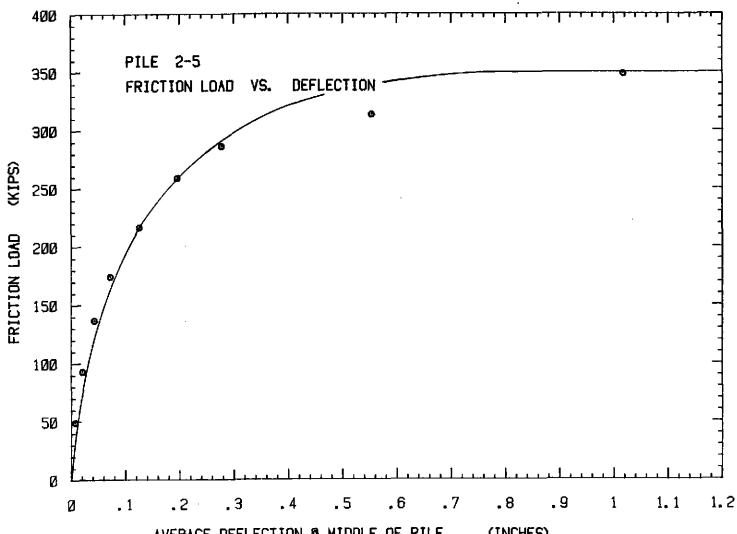

FIG. 42 - Friction Load Versus Average Deflection for Pile 2-5 (1 kip = 4.448 kN; 1 in. = 2.54 cm)

were used to determine the point quakes and the side quakes for the analysis. Appendix I contains the tables from which the Axial Deflection curves and Load Distribution curves were obtained; it also contains an example explaining how the Point Load curves and Friction Load curves were determined.

Pile Driving Data

Driving data consists of hammer information, dynamic field measurements data, and the driving records from the field. The hammer manufacturer provided the hammer information necessary to perform a wave equation analysis. The Corps of Engineers authorized the dynamic field measurements and provided data for the selected piles. The Corps of Engineers also provided the driving records.

All piles were driven with an ICE 640 diesel pile driving hammer. Table 4 gives the hammer specifications required for a wave equation analysis (Tony Last, International Construction Equipment, Inc., personal communication, 6-4-84). Fig. 43 is a schematic drawing of the hammer assembly.

Dynamic field measurements were made using the Pile Driving Analyzer developed by Goble. The parameters printed out on paper tape are:

FMAX, the maximum measured compression force at the transducer location, kips.

RSTC, the Case-Goble Method static resistance using damping (J), kips.

EMAX, the maximum value of energy transmitted past the transducer location, kip feet.

RMAX, the maximum Case-Goble Method resistance using damping kips.

TABLE 4. - ICE 640 Diesel Pile-Driving Hammer Data

Hammer Type	Closed-End
Rated Kinetic Energy	40,000 ft-lbs
Rated Equivalent Ram Stroke	79.32 in.
Distance from Anvil to Exhaust Ports	12.625 in.
Ram Weight	6000 lbs
Ram Length	91.69 in.
Ram Velocity (Calculated based on 16,470 ft-lbs of energy required to compress air in chamber from exhaust ports to anvil -- energy from gas laws.)	15.90 ft/sec
Theoretical Explosive Pressure (Calculated with ram at Bottom Dead Center)	1290 psi
Probable Explosive Pressure	1190 psi
Hammer Bore Diameter	18.00 in.
Calculated Explosive Force	303-328 kips
Anvil Weight	1415 lbs
Striker Cap Weight (To be combined with anvil weight)	580 lbs
Capblock Assembly Weight	1534 lbs
Cushion Material	6 - 1/2" thick Micarta disks w/5 - 1/8" thick aluminum plates
Cushion Diameter	10.875 in.
Calculated Cushion Stiffness	13,800 kip/in.
Cushion Coefficient of Restitution	0.8

Note: 1 ft = 0.305 m; 1 kip = 4.448 kN

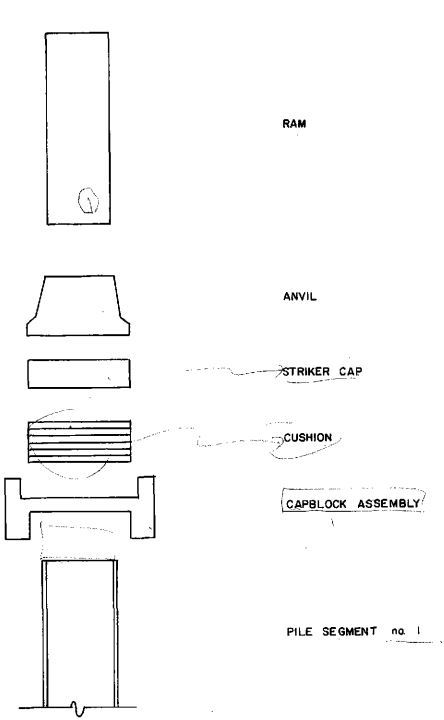

FIG. 43. - ICE 640 Diesel Pile Driving Hammer. Schematic Drawing

Table 5 gives values of the above parameters for each pile; the values were taken from the last foot of driving. RSTC and RMAX were not used in the analysis but are listed for the sake of completeness.

Fig. 44 through Fig. 47 are the driving records for the selected piles. The average driving resistance at final penetration is 32 blows/ft (147 blows/m).

TABLE 5. - Dynamic Field Measurements from the Pile Driving Analyzer

Pile No.	FMAX (kips)	RSTC (kips)	EMAX (ft-kips)	RMAX (kips)
1-3A	590	367	13.8	372
1-6	465	388	26.4	391
1-9	473	240	not available	304
2-5	469	173	10.6	244

Note: 1 kip = 4.448 kN; 1 ft-lb = 1.356 joule (Nm)

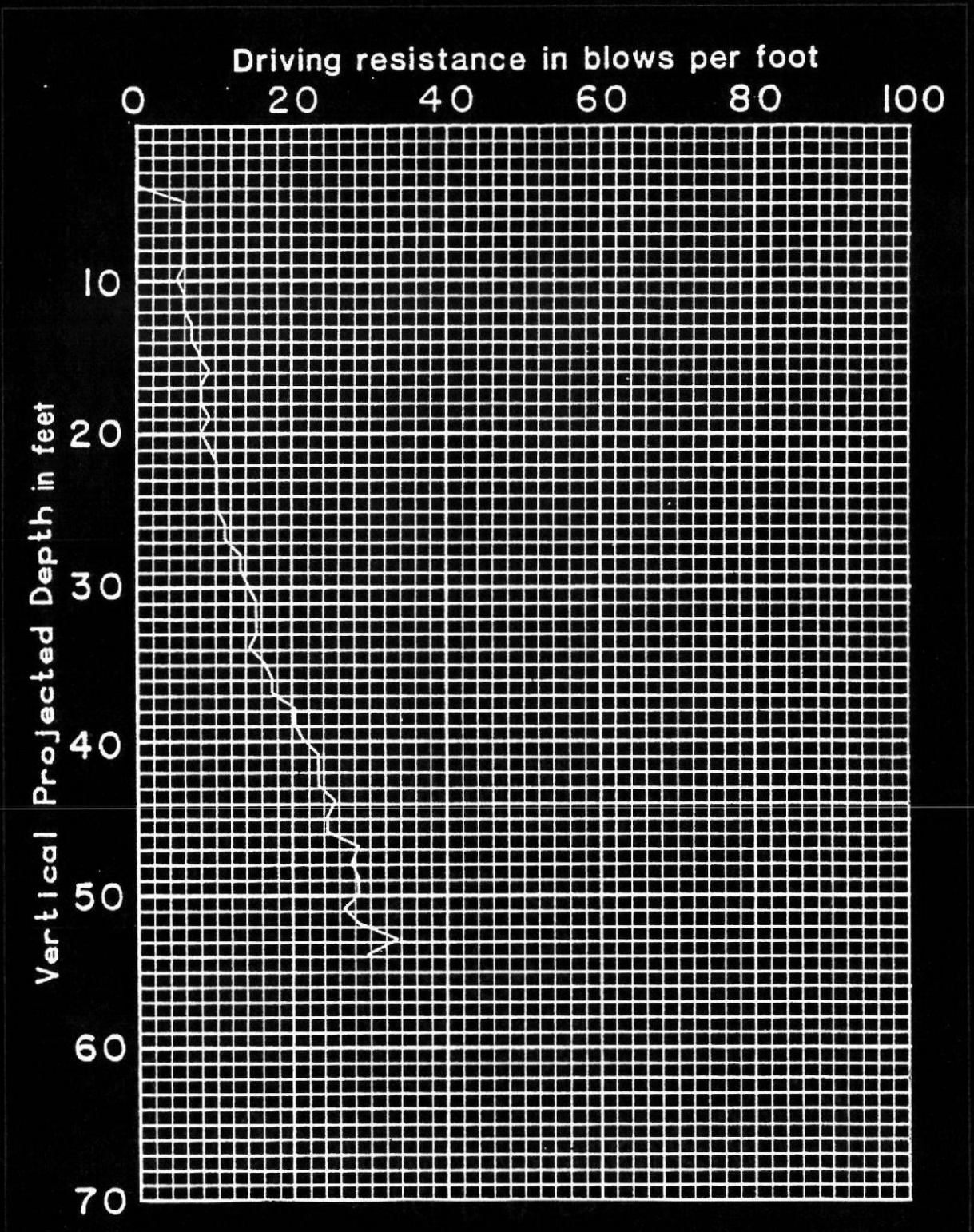

FIG. 44. - Driving Record for Pile 1-3A
(1 ft = .305 m)

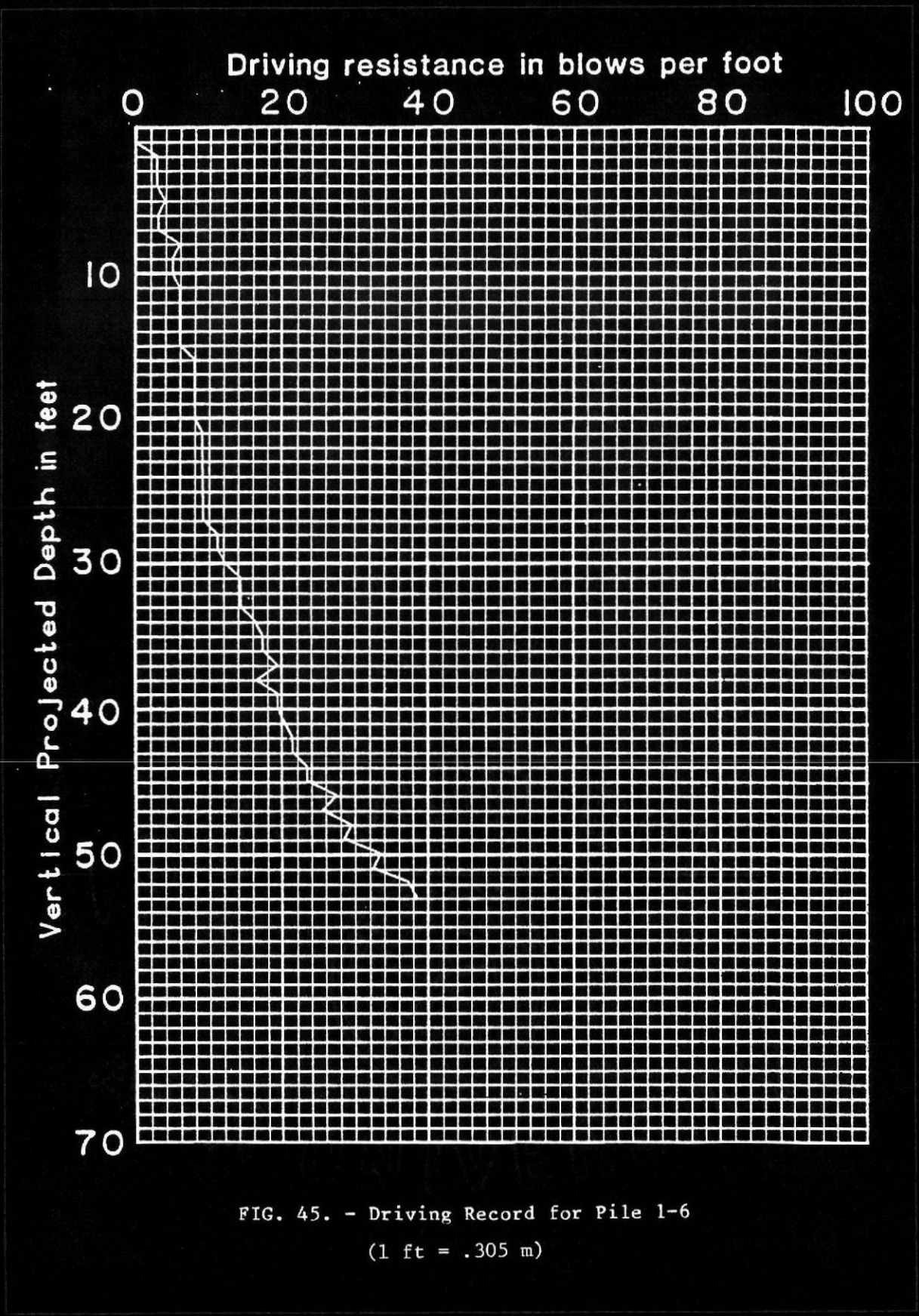

FIG. 45. - Driving Record for Pile 1-6

(1 ft = .305 m)

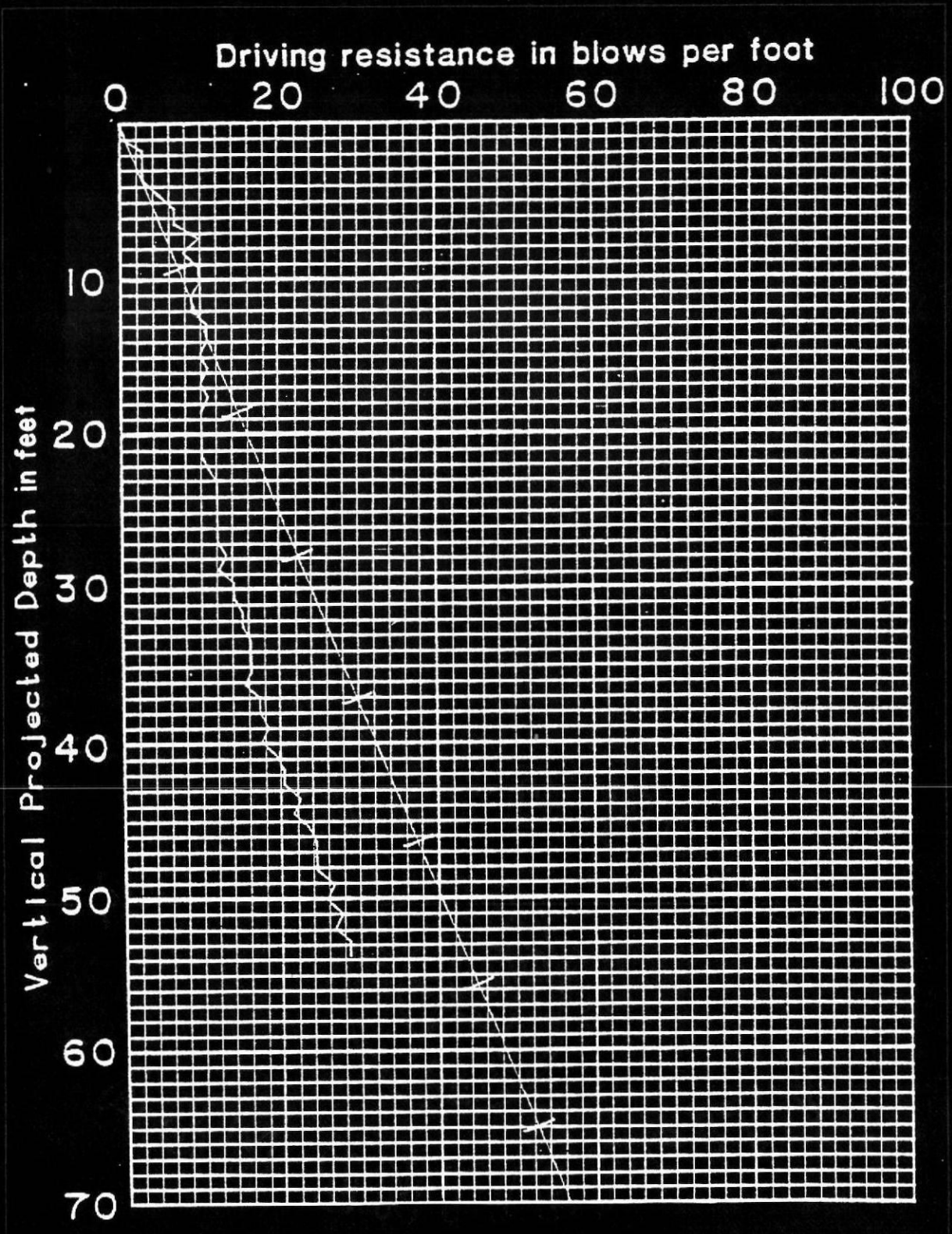

FIG. 46. - Driving Record for Pile 1-9

(1 ft = .305 m)

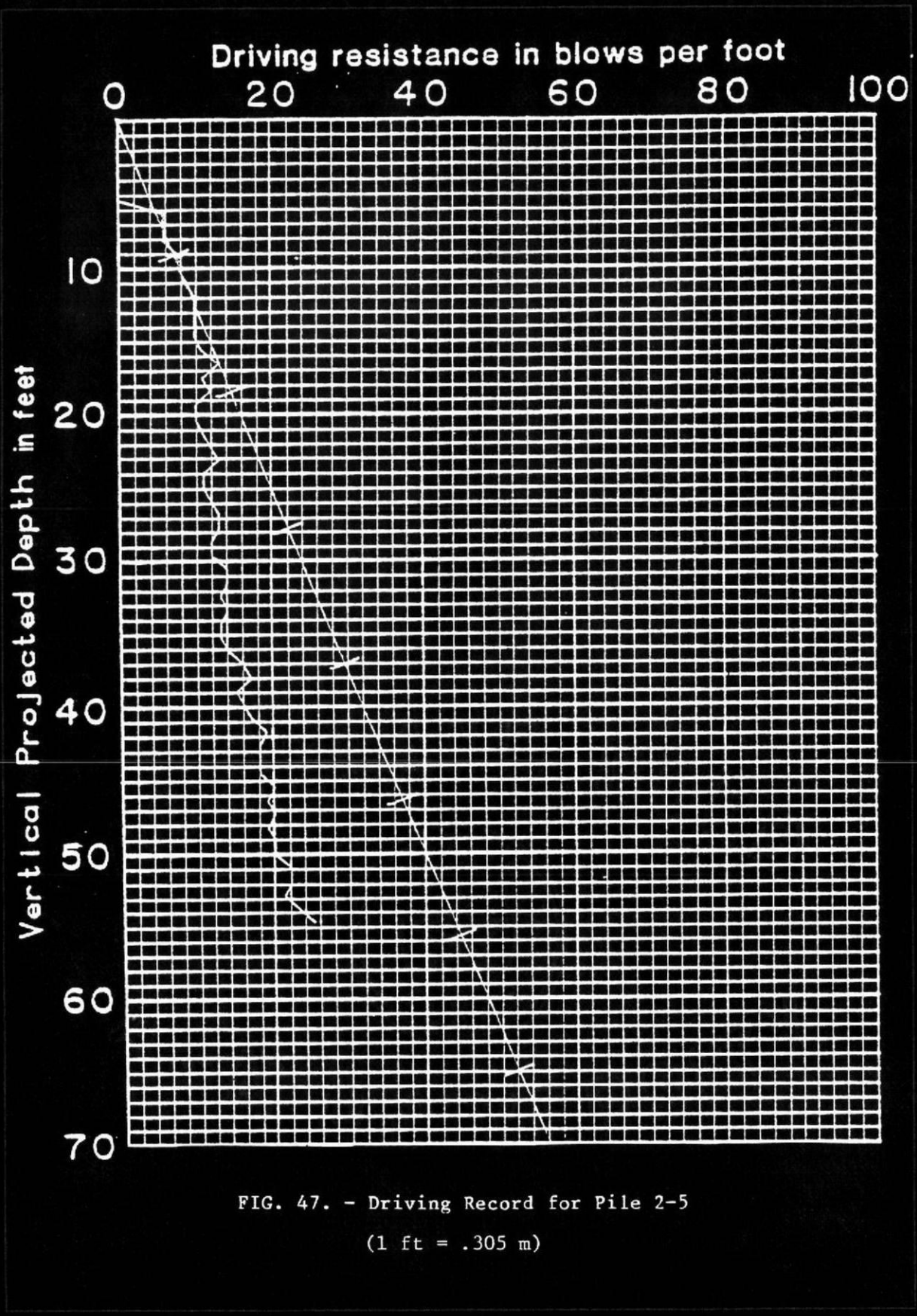

FIG. 47. - Driving Record for Pile 2-5

(1 ft = .305 m)

CHAPTER VII

LOCK & DAM NO. 26: WAVE EQUATION ANALYSIS

Objectives

The primary goal of this analysis is to determine values for the wave equation computer program input parameters, quake and damping, which represent the soil at the Lock & Dam No. 26 site. Residual stresses will be studied using data from Pile 1-3. In addition, the analysis will compare the results of selected pile driving formulas with wave equation results and static load test values. The TAMU wave equation computer program, TIDYWAVE, will be used exclusively throughout the analysis.

Determination of Quake and Damping - Overview

Quake and damping values can be determined by a regression-best fit analysis. Given the driving system data (i.e. pile, hammer), one can backfigure the quake and damping which yield a measured quantity. This measured quantity can be either the force-time curve at the pile head or the ultimate static resistance. This study answers the specific question, "What quake and damping values lead to a match between the computed ultimate static soil resistance (by the wave equation - - corresponding to the time of driving) and the measured value from the static load test?"

The method used to determine the input parameters is similar to the method described by Coyle et al. in their Texas Transportation Institute Research Report No. 125 series, Bearing Capacity for Axially Loaded Piles. Reference (8) is the summary report for that study,

and Reference (9) is a succinct presentation of their findings.

Coyle et al. were given instrumented pile load test data and a measured peak driving force at the pile head. They selected "best fit" quake values and determined the ultimate static soil resistance using the load test data. They then matched the computed peak force with the measured peak dynamic force at the pile head to eliminate uncertainty in the hammer input data. These forces were matched by varying cushion stiffness and ram velocity in the wave equation analysis. Once they obtained a force match, they varied the damping parameter J and developed a series of Ultimate Static Soil Resistance vs. Blowcount (RUT vs. N) curves. Plotting the ultimate static soil resistance at its corresponding blowcount value on the RUT vs. N curves determined the correct value of J.

Ultimate Static Resistance

The ultimate static soil resistances were taken from the Load vs. Pilehead Movement curves (Fig. 31 through Fig. 34). The ultimate static resistance is the resistance corresponding to a pile head deflection of 10 percent of the equivalent pile diameter. Piles which did not achieve this deflection did not "plunge". The equivalent pile diameter for an H-pile is:

$$d_{eq} = \sqrt{\frac{4(b_f \cdot d)}{\pi}} \qquad (20)$$

where

b_f = pile flange width, in. or cm

d = pile web depth, in. or cm

Properties for the HP 14 x 73 rolled shape from the AISC Manual of Steel Construction, Eighth Edition are:

b_f = 14.585 in. (37.06 cm)

d = 13.61 in. (34.57 cm)

The equivalent pile diameter is 15.90 in. (40.37 cm). Table 6 and Fig. 48 give the ultimate static soil resistances for each pile and the corresponding blowcount value at final penetration from the blowcount curves.

Selection of Quakes

Quake values were obtained from the Point Load vs. Point Deflection curves (Fig. 35 through Fig. 38) and the Friction Load vs. Average Deflection curves (Fig. 39 through Fig. 42). The primary consideration involved deciding whether to choose a 50% secant quake or 25% secant quake.

Secant quakes were determined in a rational and systematic manner. A secant was drawn through the point on the load-deflection curve corresponding to 25% or 50% of the maximum load on that curve. Fig. 49 is the Point Load vs. Point Deflection curve for Pile 1-3A with the 25% secant point quake shown. The 25% secant friction quake was obtained in the same manner as the point quake but from the friction load-deflection curve. Table 7 summarizes the quake values used in this analysis.

Unloading quake characteristics were determined from Fig. 34, the

TABLE 6. - Ultimate Static Soil Resistance and Corresponding Blowcount Data

Pile No.	Ultimate Static Resistance (kips)	Blowcount Value (blows/ft)
1-3A	580	34
1-6	818	38
1-9	652	29
2-5	447	25

Note: 1 kip = 4.448 kN; 1 ft = 0.305 m

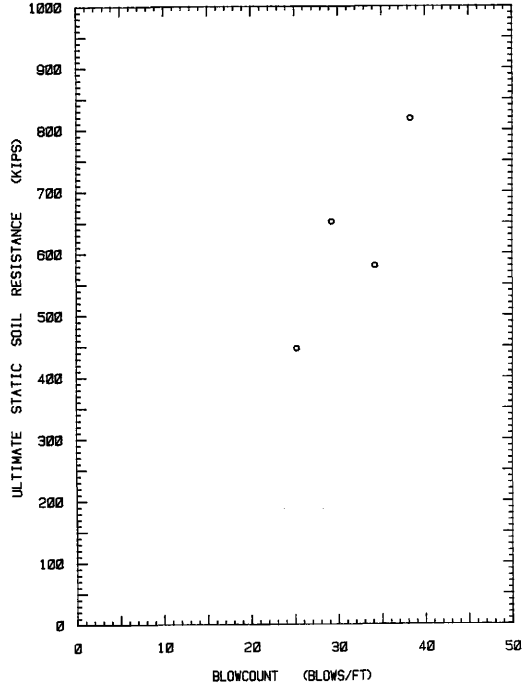

FIG. 48. - Ultimate Static Soil Resistance Versus Blowcount for Selected Piles at Lock & Dam No. 26
(1 kip = 4.448 kN; 1 ft = .305 m)

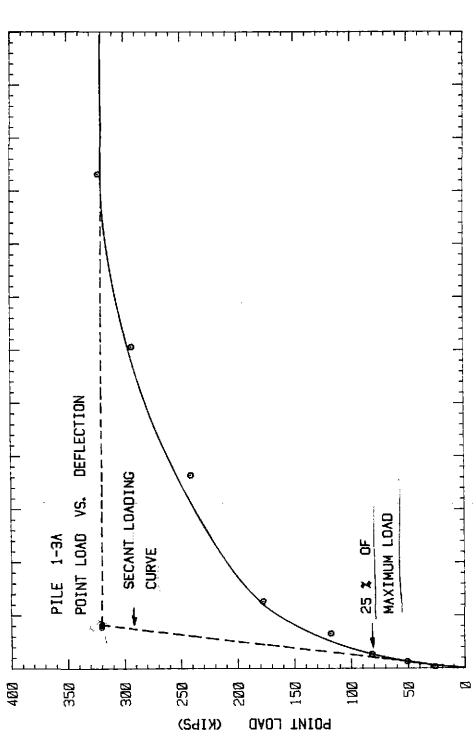

FIG. 49 - Determination of 25% Secant Quake Values (1 kip = 4.448 kN; 1 in. = 2.54 cm)

TABLE 7. - Quake Values Used for this Analysis

Pile No.	50% Secant Quakes		25% Secant Quakes	
	Q_{point} (inches)	Q_{side} (inches)	Q_{point} (inches)	Q_{side} (inches)
1-3A	0.57	0.40	0.20	0.12
1-6	0.40	(0.35)	0.24	(0.45)
1-9	0.33	0.30	0.17	0.13
2-5	0.28	0.20	0.13	0.08
Average	0.40	0.30	0.185	0.11

Unloading Quakes equal the above Loading Quake Values.

Note: 1 in. = 2.54 cm

Load vs. Pilehead Movement curve for Pile 2-5. Fig. 34 is the only curve that shows a complete load-unload-reload-unload cycle. From Fig. 34, the initial loading quake is 0.30 in. (0.762 cm)(obtained using the secant at 25 percent of ultimate load method). The first unload quake is 0.31 in. (0.787 cm). The reload quake value is 0.17 in. (0.432 cm), and the second unload quake is 0.15 in. (0.381 cm). The loading and unloading quakes are approximately equal for a cycle; however, the second cycle values are one half the first cycle values.

This phenomenon might occur because the initial load test cycle was performed 8 days after driving allowing adequate time for pore pressure dissipation or pile "set-up". The second load test cycle, on the other hand, was performed immediately after the first cycle, and pore pressures may not have had time to dissipate; the result is the stiffer, low-quake soil. Regardless of the explanation, there is an indication that, for cyclic loading, unloading quakes differ very little from the loading quakes.

For this analysis, the unloading quakes were assumed to equal the loading quakes for both point and side values.

Matching FMAX

The FMAX values listed in Table 5 are measured maximum compressive forces delivered to the pile head. Matching a measured peak force with the computed peak force from a wave equation computer program eliminates much uncertainty in the hammer input parameters; that is, there is no longer any need to guess a hammer efficiency or estimate cushion properties. Coyle et al. (9) state that matching the peak force produces reliable results.

Factors which affect the magnitude of the peak compressive force at the pile head are the ram velocity, the number of segments used to model the ram, the cushion stiffness, and the stiffness of the pile. Varying any or all of these parameters alters the computed stress wave to produce the peak force match. In this analysis, the first three parameters were varied; the pile stiffness was not changed. Also, all force match runs used the 25% secant quake values, Smith damping values, and the ultimate static soil resistance from the load test.

The first match was attempted on Pile 1-3A. The initial runs were made with the ram modeled as a single segment; unaltered input data (as suggested from the manufacturer) produced a computed peak force 26 percent greater than the measured value for this pile. The ram velocity and cushion stiffness were then decreased in increments of approximately 5 percent until measured and computed forces agreed. The force match was achieved at 81 percent of the manufacturer's calculated ram velocity and 90 percent of the calculated cushion stiffness. Varying the cushion stiffness had very little effect on the hammer force; a 5 percent change in cushion stiffness produced a 1 percent or less change in the hammer force.

The ram was then divided into three segments. A force match was achieved at 100 percent of the manufacturer's calculated ram velocity and 90 percent of the calculated cushion stiffness. (This large change due to the segmented ram supports the findings of Lowery et al. (34) in their investigation of driving stresses calculated by TAMU wave equation computer programs.) These new values were considered acceptable, and a three-segment ram was used for all subsequent

computer runs.

The FMAX values for Piles 1-6, 1-9, and 2-5 differ by only 1 percent, but they are only 71 percent of the FMAX value for Pile 1-3A. Not surprisingly, the peak force match was achieved at 75 percent of the manufacturer's computed ram velocity and 90 percent of the computed stiffness for Piles 1-6 and 2-5. Pile 1-9 was matched using 76 percent of the ram velocity. The values were accepted and were used in subsequent computer runs to develop RUT vs. N curves.

Developing the Ultimate Static Resistance versus Blowcount Curves

Engineers use RUT vs. N curves to establish pile driving acceptance criteria. Acceptance criteria will tell the pile driving contractor that "this" hammer on "this" pile in "this" soil driven to "this" minimum depth with "this" blowcount value will achieve the required static bearing capacity at the time of driving. The unknowns in a typical pile driving analysis are the hammer, the pile, and the soil information; the result of the analysis is the static bearing capacity with its corresponding blowcount value.

In this analysis, dynamic field measurements were made, so the hammer data is known. Pile data is also known. Driving records were taken, so the blowcount value is known. The ultimate static soil resistance is available from static load test results. The unknowns, then, are the soil input parameters, quake and damping. Quake values were determined from the load-deformation curves, so the analysis finally reduces to selecting proper damping parameter values.

Ideally, the analysis could be made by specifying only one value of soil resistance (the ultimate value from the load test) and varying

the damping parameter until the wave equation computer program's calculated blowcount value matches the blowcount value from the driving record.

A more useful method of analysis, however, is to develop complete RUT vs. N curves for a series of damping values. The curves for a particular pile can be plotted together, as a family, and the point representing the ultimate static soil resistance and its corresponding blowcount value can be plotted on this family of curves. The correct damping value is readily apparent, as well as trends in the results.

This analysis developed a series of RUT vs. N curves. The damping values chosen were:

J_{point} = 0.00 sec/ft (0.0 sec/m)
0.05 sec/ft (0.164 sec/m)
0.15 sec/ft (0.492 sec/m)
0.30 sec/ft (0.984 sec/m)

$J_{side} = 1/3\ J_{point}$

Multiple hammer blows were used, so permanent set was calculated based on the complete time history of pile tip movement rather than by maximum displacement minus quake. Specifically, the analysis modeled 5 consecutive hammer blows, and permanent set was the difference in the final displacements of the fourth and fifth blows. Typically, 600 iterations (time step intervals) were calculated for each blow.

RUT values were chosen in 100 kip (445 kN) increments ranging from 100 kips (445 kN) to a value approximately 100 kips (445 kN) greater than the maximum static resistance from the load test. The

ratio of point resistance to total resistance (RUP/RUT) for each pile was determined from the Load Distribution vs. Pile Depth curves (see Appendix I) using the maximum applied load value for RUT. This ratio was held constant for all subsequent increments of RUT; the friction resistance (RUT minus RUP) was assumed to be uniformly distributed.

Pile 1-3A was analyzed using both the 50% secant quakes and the 25% secant quakes. Pile 1-6, Pile 1-9, and Pile 2-5 were analyzed using only the 25% secant quake values. The results of the analysis are presented in the next section.

Results

Fig. 50 is a plot of the RUT vs. N curves for Pile 1-3A. The 50% secant quakes were used to develop these curves. Table 8 is a complete numerical tabulation of the results plotted on Fig. 50. The closest blowcount correlation is for zero damping, but this value is 100 percent too high.

Fig. 51 and Table 9 are the results for Pile 1-3A obtained using the 25% secant quake values. The closest blowcount correlation is also for zero damping, but is considerably closer. The calculated blowcount is 40 percent larger than the measured value for this pile.

Pile 1-6 is unusual because of its comparatively high static soil resistance and its abnormally large side quake value. The analysis was done only for damping values of 0.0 sec/ft and 0.30 sec/ft (0.984 sec/m), and Table 10 presents the results. Computer runs were made for RUT values ranging from 100 kips to 1000 kips

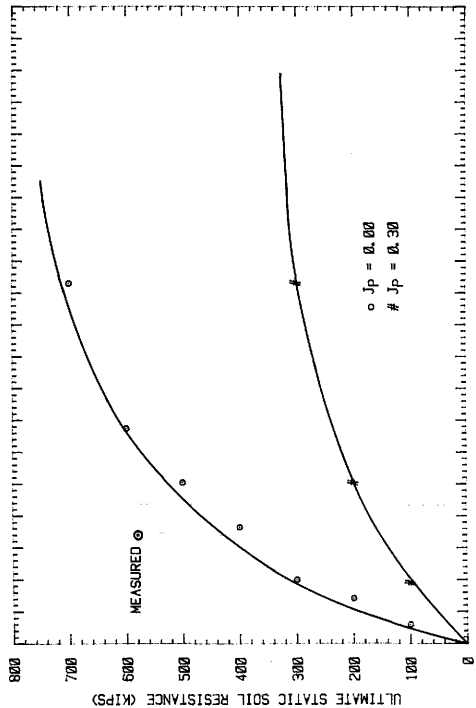

FIG. 50 - RUT Versus N for Pile 1-3A Using 50% Secant Quakes (1 kip = 4.448 kN; 1 ft = .305 m)

TABLE 8. - RUT and Blowcount Results for Pile 1-3A Using 50% Secant Quakes

J_p = 0.0 sec/ft		J_p = 0.30 sec/ft	
N (blows/ft)	RUT (kips)	N (blows/ft)	RUT (kips)
6.0	100	19.1	100
14.2	200	50.4	200
20.0	300	113.2	300
36.5	400	2000	400
50.4	500	3000	500
67.4	600	4000	600
112.7	700	6000	700

Note: 1 ft = 0.305 m; 1 kip = 4.448 kN

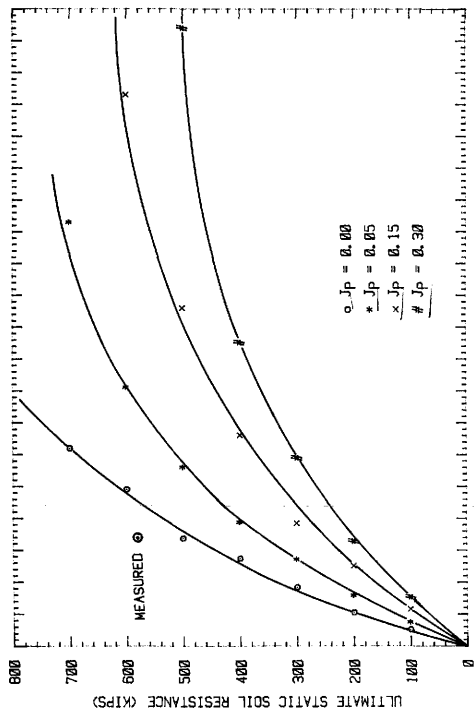

FIG. 51 - RUT Versus N for Pile 1-3A Using 25% Secant Quakes (1 kip = 4.448 kN; 1 ft = .305 m)

TABLE 9. - RUT and Blowcount Results for Pile 1-3A Using 25% Secant Quakes

J_p = 0.0 sec/ft		J_p = 0.05 sec/ft		J_p = 0.15 sec/ft		J_p = 0.30 sec/ft	
N (blows/ft)	RUT (kips)	N (blows/ft)	RUT (kips)	N (blows/ft)	RUT (kips)	N (blows/ft)	RUT (kips)
5.2	100	7.5	100	11.5	100	15.3	100
10.5	200	15.9	200	25.1	200	32.8	200
18.4	300	27.2	300	38.5	300	59.0	300
27.4	400	38.8	400	66.1	400	95.2	400
33.7	500	56.1	500	106.2	500	193.5	500
49.1	600	81.1	600	173	600	631	600
62.0	700	133.3	700	353	700		700

Note: 1 ft = 0.305 m; 1 kip = 4.448 kN

TABLE 10. - RUT and Blowcount Results for Pile 1-6 Using 25% Secant Quakes

J_p = 0.0 sec/ft		J_p = 0.30 sec/ft	
N (blows/ft)	RUT (kips)	N (blows/ft)	RUT (kips)
10.5	100	25.4	100
36.9	200	116	200
59.4	300	857	300
150	400	ND	400
358	500	ND	500
ND	600	ND	600
ND	700	ND	700
ND	800	ND	800
ND	900	ND	900
ND	1000	ND	1000

Note: ND indicates negative calculated pile displacement; 1 ft = 0.305 m; 1 kip = 4.448 kN

(445 kN to 4450 kN), but less than half of these runs produced meaningful information. Blowcount values marked "ND" could not be calculated because the computer solution showed the pile experiencing negative displacement. This means that the pile bounced out of the ground with each blow instead of penetrating further. The reason for this behavior is most likely the large side quake value used for the analysis. The Friction Load vs. Deflection curve (Fig. 40) justifies this quake, however. No further attempt was made to correlate static load bearing capacity with blowcount for Pile 1-6.

Fig. 52 and Table 11 present the results for Pile 1-9. The results are consistent with those of Pile 1-3A in that zero damping produces the best blowcount correlation. The results are not close, however. The calculated blowcount value is 5 times larger than the measured value.

The blowcount value for Pile 2-5 also correlates using zero damping. The results are better than those for Pile 1-9, but the calculated blowcount value is still 2.4 times too large. Fig. 53 and Table 12 present the results for Pile 2-5.

The first paragraphs of this section present the results in terms of: "Given a value of static soil resistance, the corresponding computed blowcount is _____." The computed blowcount is then compared with the measured value. An equally valid way to present the results is to say: "Given the following blowcount value, the computed ultimate static soil resistance is _____." The computed ultimate value is then compared to the measured static soil

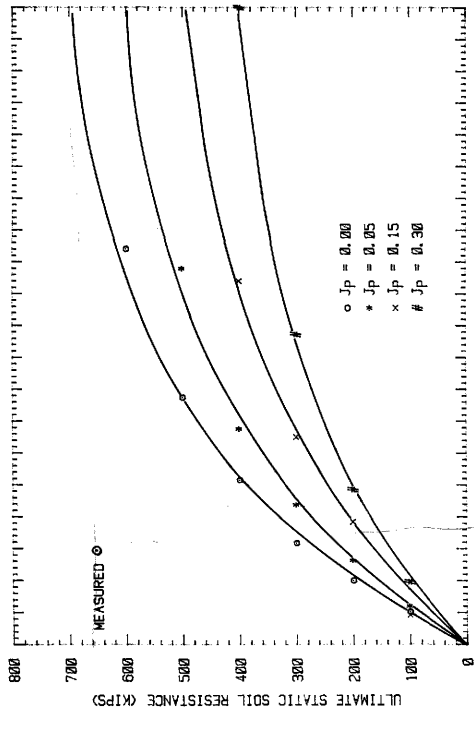

FIG. 52 – RUT Versus N for Pile 1-9 Using 25% Secant Quakes (1 kip = 4.448 kN; 1 ft = .305 m)

TABLE 11. - RUT and Blowcount Results for Pile 1-9 Using 25% Secant Quakes

J_p = 0.0 sec/ft		J_p = 0.05 sec/ft		J_p = 0.15 sec/ft		J_p = 0.30 sec/ft	
N (blows/ft)	RUT (kips)	N (blows/ft)	RUT (kips)	N (blows/ft)	RUT (kips)	N (blows/ft)	RUT (kips)
10.2	100	12.0	100	9.2	100	19.6	100
20.0	200	26.3	200	38.4	200	48.5	200
31.7	300	43.8	300	65.0	300	97.2	300
51.5	400	67.6	400	114	400	200	400
77.4	500	118	500	211	500	480	500
124	600	203	600	462	600	1500	600
207	700	369	700	1846	700	2000	700

Note: 1 ft = 0.305 m; 1 kip = 4.448 kN

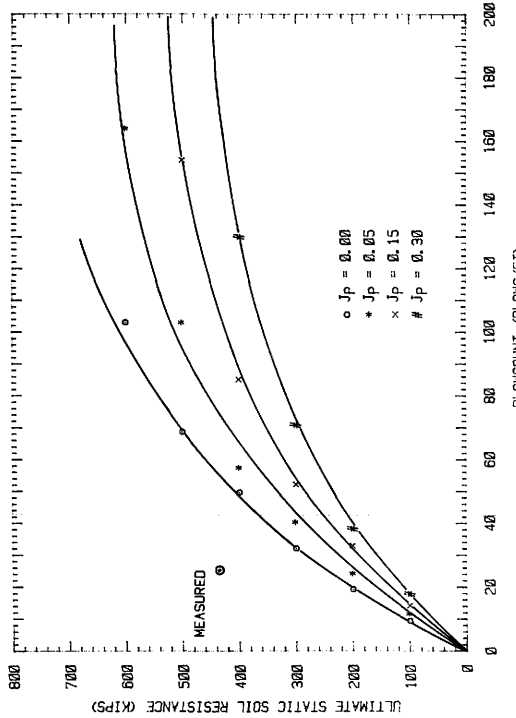

FIG. 53 - RUT Versus N for Pile 2-5 Using 25% Secant Quakes (1 kip = 4.448 kN; 1 ft = .305 m)

TABLE 12. - RUT and Blowcount Results for Pile 2-5 Using 25% Secant Quakes

J_p = 0.0 sec/ft		J_p = 0.05 sec/ft		J_p = 0.15 sec/ft		J_p = 0.30 sec/ft	
N (blows/ft)	RUT (kips)	N (blows/ft)	RUT (kips)	N (blows/ft)	RUT (kips)	N (blows/ft)	RUT (kips)
9.5	100	11.7	100	14.3	100	17.9	100
19.3	200	24.3	200	32.9	200	38.3	200
32.1	300	40.4	300	52.2	300	70.8	300
49.7	400	57.4	400	85.1	400	130	400
68.6	500	103	500	154	500	261	500
103	600	164	600	308	600	632	600

Note: 1 ft = 0.305 m; 1 kip = 4.448 kN

resistance. This method of presenting results is less volatile than the blowcount method even though the data is the same. Engineers use this method more often because they typically know blowcount values and desire to know ultimate load bearing capacity information.

Table 13 presents the results in terms of static soil resistances. For Pile 1-3, the computed values using the 50% secant quakes and 25% secant quakes are 69 percent and 86 percent of the measured value. The computed value for Pile 1-9 is 43 percent of the measured static resistance, which is quite low. For Pile 2-5, the computed resistance is 58 percent of the measured load test value.

Discussion

The results overwhelmingly show that the best damping value to produce a correlation of static bearing capacity with blowcount is zero. The analysis of each pile, regardless of the quake used, substantiates this value. Zero damping is consistent with the more recent recommendations cited in the literature review - e.g., CRWU (by Holloway), Beringen, and Heerema.

Sporadically large differences between measured and computed values blight the credibility of the zero damping trend, however. There are several possible explanations for deviations in the results.

First, the data is subject to uncertainty. This statement applies to all data: dynamic field measurements, driving records, and load test data. Limitations are inherent in any type of measuring equipment, and all equipment is subject to malfunction.

TABLE 13. - Ultimate Static Soil Resistance
Calculated by the Wave Equation for Zero Damping

Pile 1-3A (N = 34 blows/ft)	
RUT, static load test	580 kips
RUT, wave equation, 50% Secant quake	400 kips
RUT, wave equation, 25% Secant quake	500 kips
Pile 1-9 (N = 29 blows/ft)	
RUT, static load test	652 kips
RUT, wave equation, 25% Secant quake	280 kips
Pile 2-5 (N = 25 blows/ft)	
RUT, static load test	447 kips
RUT, wave equation, 25% Secant quake	260 kips

Note: 1 ft = 0.305 m; 1 kip = 4.448 kN

Certainly, human error is a possibility. There are a number of ways to introduce inconsistency and uncertainty in a load test, ranging from the operator to the equipment to the physical conditions of a particular test. Of course, every attempt was made to produce reliable, accurate data, but raw data is a possible source of error in this analysis.

Second, the analysis method and its many components are subject to uncertainty. For example, even though the procedure used to determine ultimate load is standard, it could be wrong. Loading quakes were chosen in a rational and systematic manner, and the quake values are consistent with those found in literature. Nevertheless, there was a wide range of possible values, and the "correct" quake could easily be different from the chosen secant value. Unloading quakes are a possible source of error. Another source of uncertainty is that this analytsis matched peak compressive forces at the pile head. Complete force-time data would have provided a more certain match, because a complete force-time curve models the actual shape of the stress wave as well as the peak force value. Choosing J_{side} equal 1/3 J_{point} is another analysis assumption that could produce error. Althogh all facets of the analysis were based on some precedent, the analysis method itself could introduce and propogate errors.

Third, the entire wave equation method of pile driving analysis is subject to uncertainty. Wave equation theory is based on certain assumptions as discussed in Chapter II. The numerical solution is approximate rather than exact; Chapter III and Chapter IV discuss

the numerical solution and the various programs written to solve it. Computer soil models are also a possible source of error; Chapter V presents an in-depth study of both static and dynamic soil models. Obviously, there are several ways in which the wave equation method can introduce errors in the analysis.

Explanations of variations in the results should not be construed as saying the analysis is unscientific or haphazard. On the contrary, the wave equation method is the best available tool for pile driving analysis. There is great opportunity for variability in the analysis method, but the method is consistent, rational rational, and well documented. Data acquisition was accomplished using the best possible procedures. In short, the analysis used available resources to their fullest extent to produce the best possible results.

This study illuminates areas for further research, and it also points out "problem areas" which should be approached with care in subsequent analyses. Chapter VIII presents these recommendations. The following two sections of this chapter describe "offshoots" of the analysis: residual stress effects and dynamic pile driving formula comparisons.

Residual Stress Analysis

Tucker (48) presents an in-depth study of residual stresses. He discusses the basic considerations of the phenomenon and also describes procedures for obtaining residual stresses from load tests, for obtaining residual stresses from the wave equation, and for making residual stress predictions. With Tucker's work as background information, this analysis determines the measured

residual stress in Pile 1-3, computes residual stresses by the wave equation, and makes a residual stress prediction based on Tucker's correlation.

The residual stress analysis was performed on Pile 1-3 because Pile 1-3 is the only selected pile which was tested in tension; an instrumented tension test is required to obtain a measured value for residual point load. The tables from which the Axial Deflection and Load Distribution vs. Pile Depth curves for the tension test (Test No. 1-3B) were determined are in Appendix I. The residual point load is read directly from the Load Distribution vs. Pile Depth curve. It is the load at a depth of 49.65 ft (14.83 m) for the applied load of 66 tons (587 kN). This measured value is 34.33 tons (69 kips)(305 kN).
I. The residual point load is read directly from the Load Distribution vs. Pile Depth curve. It is the load at a depth of 49.65 ft (14.83 m) for the applied load of 66 tons (587 kN). This measured value is 34.33 tons (69 kips)(305 kN).

A wave equation analysis was done for comparison with the measured value. The same computer runs used in the static bearing capacity vs. blowcount correlation are used for residual stress calculations. The residual stress analysis requires more iterations per blow to properly determine the residual point load, however. This is especially true for low damping values and low soil resistances; the computer results for J = 0.0 sec/ft and 0.05 sec/ft (0.164 sec/m) were rerun using 1500 iterations/blow rather than 600 iterations/blow.

Fig. 54 and Table 14 are the results obtained by using the 50% secant quakes. The unique behavior of the 0.30 sec/ft (0.984 sec/m)

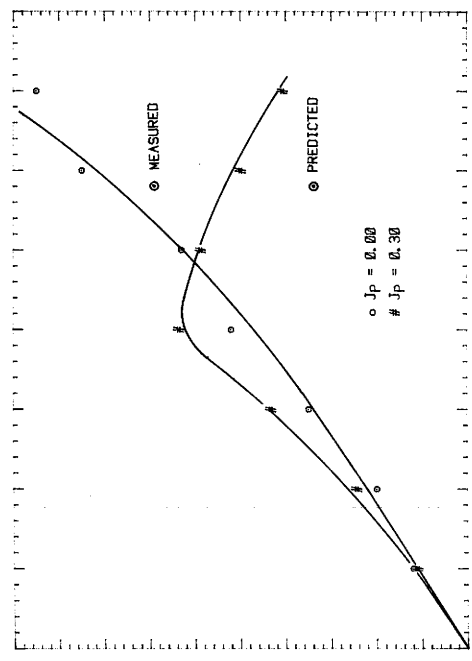

FIG. 54. - Residual Point Load Results for Pile 1-3 Using 50% Secant Quakes (1 kip = 4.448 kN)

TABLE 14. - Residual Point Load Results for Pile 1-3 Using 50% Secant Quakes

J_p = 0.0 sec/ft		J_p = 0.30 sec/ft	
Residual Point Load (kips)	RUT (kips)	Residual Point Load (kips)	RUT (kips)
12	100	11	100
20	200	24	200
35	300	43	300
52	400	64	400
63	500	59	500
85	600	50	600
95	700	41	700

Note: 1 ft = 0.305 m; 1 kip = 4.448 kN

damping curve could be attributed to the extremely high calculated blowcounts (see Table 8). Briaud et al. (6) reported the same phenomenon in an analysis with similarly high blowcounts. Fig. 55 and Table 15 are the results obtained by using the 25% secant quake values.

The computed values agree quite well with the measured value. For the 50% secant quake, the computed value is 20 percent too high. The computed value using the 25% secant quake is 45 percent too high. Both of these comparisons are for the zero damping curve. In addition to close comparisons, the following trends are present in the results: increasing damping increases residual point load, and increasing quake decreases residual point load.

Tucker's predictive method is based on an empirical β parameter (48). He predicts a residual point pressure and states that this pressure is primarily a function of pile length and relative stiffness between the soil and the pile. In equation form:

$$q_{res} = 5.57\ L\beta \tag{21}$$

where

q_{res} = residual point pressure, tsf

L = pile length, ft

$\beta = \sqrt{\frac{K_\tau P}{A E_p}}$, consistent units required

$K_\tau = 5.01\ (N_{side})^{0.27}$, tsf/in., the initial tangent modulus of the Friction Load vs. Average Deflection curve.

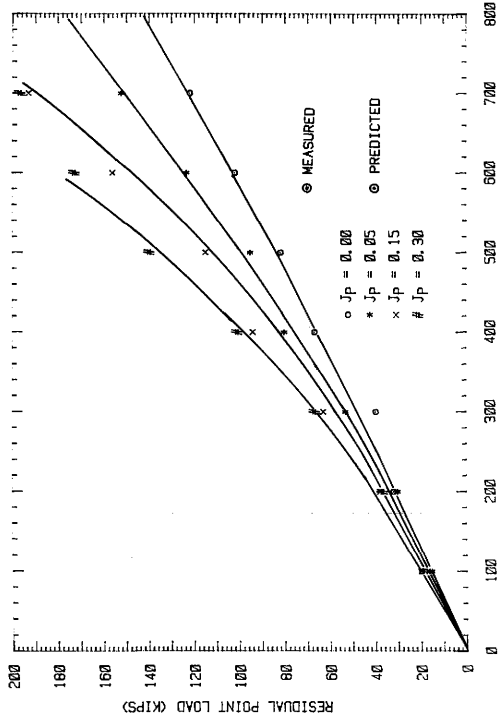

FIG. 55. - Residual Point Load Results for Pile I-3 Using 25% Secant Quakes (1 kip = 4.448 kN)

TABLE 15. - Residual Point Load Results for Pile 1-3 Using 25% Secant Quakes

J_p = 0.0 sec/ft		J_p = 0.05 sec/ft		J_p = 0.15 sec/ft		J_p = 0.30 sec/ft	
Residual Point Load (kips)	RUT (kips)	Residual Point Load (kips)	RUT (kips)	Residual Point Load (kips)	RUT (kips)	Residual Point Load (kips)	RUT (kips)
20	100	15	100	20	100	17	100
32	200	30	200	38	200	37	200
40	300	53	300	63	300	67	300
67	400	80	400	94	400	101	400
82	500	95	500	115	500	140	500
102	600	123	600	156	600	173	600
122	700	152	700	193	700	197	700

Note: 1 ft = 0.305 m; 1 kip = 4.448 kN

N_{side} = weighted average of the uncorrected SPT blowcount per foot of penetration along the shaft of the pile.

P = perimeter of the pile, ft.

E_p = modulus of elasticity of the pile, tsf.

A = cross-sectional area of the pile, ft^2

For this analysis:

L = 54 ft

N_{side} = 25 (from Fig. 22)

K_T = 11.947 tsf/in. = 143.4 t/ft^3

P = 4.70 ft

A = 21.4 in. = 0.1486 ft^2

E = 29,000 ksi = 2,088,000 tsf

β = 0.0466

q_{res} = 14.0 tsf

Q_{res} = 19.3 tons (38.6 kips)(172 kN)

The predicted residual point load is 44 percent lower than the measured value, and is approximately 57 percent lower than the computed wave equation results.

In summary, the residual stress analysis shows good agreement between the load test and the wave equation values, while Tucker's method gives a predicted value which is low. The wave equation residual stress analysis substantiates the static bearing capacity analysis in that zero damping produces the best correlation.

Dynamic Pile-Driving Formulas

This analysis compares three dynamic pile-driving formulas with

the wave equation solution and static load test results. The selected formulas are the Engineering News, Danish, and Gates formulas. Olson and Flaate (37) used these formulas in their correlations for friction piles in sands. The formulas and their recommended factors of safety (F.S.) are as follows. Notation is by Olson and Flaate:

Engineering News (use F.S. = 6)

$$Q_c = \frac{e_h E_n}{S + 0.1} \qquad (22)$$

Danish (use F.S. = 3 to 6)

$$Q_c = \frac{e_h E_n}{S + \sqrt{\frac{e_h E_n L}{2AE}}} \qquad (23)$$

Gates (use F.S. = 3)

$$Q_c = 5.6 \sqrt{e_h E_n} \log (10/S) \qquad (24)$$

A = pile cross-sectional area

e_h = hammer efficiency

E = Young's modulus for pile

E_n = nominal energy of pile hammer

L = pile length

Q_c = calculated ultimate pile capacity

S = average pile penetration (set)

The Engineering News and *Danish* formulas use any consistent set of units, but the Gates formula, as shown, requires units of inches and tons. The quantity $e_h E_n$ is the energy delivered to the pile head. For this analysis, the quantity was taken as the measured value, EMAX, listed in Table 5. EMAX was not mesured for Pile 1-9, but an average of the other values was assumed for this pile. The set is the inverse of the final blowcount value listed in Table 6.

Table 16 presents the results of the dynamic pile-driving formula analysis alongside wave equation results and measured ultimate static bearing capacities. The table lists ultimate values as well as design values; design values are the ultimate values divided by a suggested factor of safety. (For comparison purposes, a factor of safety of 2 was assumed for the load test and wave equation methods.) The Engineering News formula more closely matches ultimate values, but the Gates formula provides a closer match for design purposes. All of the pile driving formula results are conservative.

Summary

This chapter presented a wave equation analysis as performed on the data from Lock & Dam No. 26. The first seven sections of this chapter described the primary objective, a correlation of ultimate static soil resistance with blowcount to determine damping, in detail. The following two sections on residual stresses and pile driving formulas are secondary considerations and were presented with little background information. This chapter also stated and discussed results.

TABLE 16. - Dynamic Pile Driving Formula Results

Method or Formula	Ultimate Resistance (kips)				Design Resistance (kips)			
	Pile 1-3A	Pile 1-6	Pile 1-9	Pile 2-5	Pile 1-3A	Pile 1-6	Pile 1-9	Pile 2-5
Static Load Test (use FS = 2)	580	818	652	447	290	409	326	224
Wave Equation (use FS = 2)	500	-	280	260	250	-	140	130
ENR Formula (use FS = 6)	366	762	395	219	61	127	66	37
Danish Formula (use FS = 3 to 6)	256	441	270	170	85-43	147-74	90-45	57-28
Gates Formula (use FS = 3)	296	423	312	236	99	141	104	79

Note: 1 kip = 4.448 kN

CHAPTER VIII

CONCLUSIONS

Conclusions

This report describes a standard wave equation soil parameter correlation of ultimate static soil resistance and blowcount. This study is unique, however, in that the soil is gravel; no published work is currently available on wave equation analyses of piles in gravel. The significant findings of the analysis are:

1. The Smith damping parameter value that leads to the best correlation between the ultimate static resistance at the time of driving (calculated by the wave equation) and the measured ultimate static resistance from the load tests for the sandy gravel at Lock & Dam No. 26 is $J_{point} = J_{side} = 0$.
2. A systematic method to select quake from static load test Load vs. Deflection curves was used. It consists of drawing a secant through the point corresponding to 25 percent of the maximum load on the Load vs. Deflection curve. The average of the quake values are:

   $Q_{point} = 0.185$ in. (0.470 cm)

   $Q_{side} = 0.11$ in. (0.279 cm)
3. A segmented ram produces significantly smaller driving stresses than those produced by a one-segment ram.
4. Wave equation residual point load values correlate well with the measured value.
5. Increased damping tends to increase the calculated residual point load, all other things held constant.

6. Increased quake tends to decrease the calculated residual point load, all other things held constant.
7. All of the pile-driving formulas used in this study gave conservative results.

Recommendations for Further Study

The following recommendatons provide some general guidelines for continued work in this area of study:

1. Instrumented load test data is invaluable. Even though the contracted purpose of a load test may not require a plunging failure, all piles being tested should be load-tested to failure in order to make the tests useful for wave equation analysis purposes.
2. Cyclic load tests at ultimate load are necessary to provide unload quake information.
3. Complete force-time data should be taken when possible.

REFERENCES

1. Authier, J. and Fellenius, B. H., "Quake Values Determined from Dynamic Measurements," Proceedings, International Seminar on the Application of Stress-Wave Theory on Piles, Stockholm, June 1980, Edited by H. Bredenberg, A. A. Balkema, Publisher, Rotterdam, 1981, pp. 197-216.

2. Authier, J. and Fellenius, B. H., "Wave Equation Analysis and Dynamic Monitoring of Pile Driving," Civil Engineering for Practicing and Design Engineers, Vol. 2, No. 4, July/August 1983, pp. 382-407.

3. Bossard, A. and Corte, J.-F., "Le Programme de Calcul BATLAB Pour L'analyse du Batlage des Pieux," Bulletin de Liaison des Laboratoires des Ponts et Chaussees, No. 128, November/December 1983, pp. 35-46.

4. Briaud, J.-L. and Tucker, L. M., "Piles in Sand - A Method Including Residual Stresses," accepted for publication in the Journal of Geotechnical Engineering, ASCE, 1984.

5. Briaud, J.-L. and Tucker, L. M., "Residual Stresses in Piles and the Wave Equation," Symposium on Deep Foundations, ASCE National Convention, San Francisco, 1984.

6. Briaud, J.-L., Tucker, L. M., Lytton, R. L., and Coyle, H. M., "Behavior of Piles and Pile Groups in Cohesionless Soils," FHWA Report No. FHWA/RD-82-38, May 1983.

7. Chan, P. C., Hirsch, T. J., and Coyle, H. M., "A Laboratory Study of Dynamic Load-Deformation and Damping Properties of Sands Concerned with a Pile-Soil System," Texas Transportation Institute, Piling Behavior Research, Research Report No. 33-7, Texas A&M University, June 1967.

8. Coyle, H. M., Bartoskewitz, R. E., and Berger, W. J., "Bearing Capacity Prediction by Wave Equation Analysis - State-of-the-Art," Texas Transportation Institute, Bearing Capacity for Axially Loaded Piles Research, Research Report No. 125-8F (Final), Texas A&M University, August 1973.

9. Coyle, H. M., Foye, R., Jr., and Bartoskewitz, R. E., "Wave Equation Analysis of Instrumented Test Piles," Preprint, 5th Annual Offshore Technology Conference, Houston, Texas, Paper No. 1892, May 1973.

10. Coyle, H. M. and Gibson, G. C., "Empirical Damping Constants for Sands and Clays," Journal of the Soil Mechanics and Foundations Division, ASCE, Vol. 96, No. SM3, Proc. Paper 7296, May 1970, pp. 949-965.

11. Cummings, A. E., "Dynamic Pile Driving Formulas," Contributions to Soil Mechanics 1925-1940, Boston Society of Civil Engineers, Boston, Mass., 1940, pp. 392-413.

12. Dolwin, J. and Poskitt, T. J., "An Optimization Method for Pile Driving Analysis," Proceedings, 2nd International Conference on Numerical Methods in Offshore Piling, Austin, Texas, 1982, pp. 91-106.

13. Dover, A. R., Ping, W.C.V., and Locke, G. E., "Parametric Study on Driveability of Large Piles," Proceedings, 2nd International Conference on Numerical Methods in Offshore Piling, Austin, Texas, 1982, pp. 49-90.

14. Dunlap, D. D., "The Effects of Repetitive Loadings on the Shearing Strength of a Cohesionless Soil," thesis submitted to the Graduate College of the Agricultural and Mechanical College of Texas, May 1959, unpublished.

15. Forehand, P. W. and Reese, J. L., "Prediction of Pile Capacity by the Wave Equation," Journal of the Soil Mechanics and Foundations Division, ASCE, Vol. 90, No. SM2, Proc. Paper 3820, March 1964, pp. 1-26.

16. Gibson, G. C. and Coyle, H. M., "Soil Damping Constants Related to Common Soil Properties in Sands and Clays," Texas Transportation Institute, Bearing Capacity for Axially Loaded Piles Research, Research Report No. 125-1, Texas A&M University, September 1968.

17. Goble, G. G., Likins, G. E., Jr., and Rausche, F., "Bearing Capacity of Piles from Dynamic Measurements," Ohio Department of Transportation Report No. OHIO-DOT-05-75, Final Report, March 1975.

18. Goble, G. G. and Rausche, F., "Pile Driveability Predictions by CAPWAP," Proceedings, Conference on Numerical Methods in Offshore Piling, The Institute of Civil Engineers, London, 1980, pp. 29-36.

19. Goble, G. G. and Rausche, F., "Wave Equation Analysis of Pile Driving," WEAP Program, Volume II: User's Manual, FHWA Report No. IP-76-14.2, July 1976.

20. Goble, G. G., Rausche, F., and Likins, G. E., Jr., "The Analysis of Pile Driving - A State-of-the-Art," Proceedings, International Seminar on the Application of Stress-Wave Theory on Piles, Stockholm, June 1980, Edited by H. Bredenberg, A. A. Balkema, Publisher, Rotterdam, 1981, pp. 131-162.

21. Heerema, E. P., "Dynamic Point Resistance in Sand and in Clay, for Pile Driveability Analysis," Ground Engineering, Vol. 14, No. 6, September 1981.

22. Heerema, E. P., "Relationships Between Wall Friction, Displacement Velocity and Horizontal Stress in Clay and in Sand, for Pile Driveability Analysis," Ground Engineering, Vol. 12, No. 1, January 1979.

23. Hirsch, T. J., Carr, L., and Lowery, L. L., Jr., "Pile Driving Analysis - Wave Equation User's Manual," TTI Program, Volume 1: Background, FHWA Report No. IP-76-13.1, April 1976.

24. Hirsch, T. J., Carr, L., and Lowery, L. L., Jr., "Pile Driving Analysis - Wave Equation User's Manual," TTI Program, Volume II: Computer Program and Sample Problems, FHWA Report No. IP-76-13.2, April 1976.

25. Hirsch, T. J., Lowery, L. L., Jr., Coyle, H. M., and Samson, C. H., Jr., "Pile Driving Analysis by One-Dimensional Wave Theory: State-of-the-Art," Highway Research Record 333, Highway Research Board, Washington, D.C., 1970, pp. 33-54.

26. Holloway, D. M., "User's Manual for DUKFOR: A Computer Program for Analyses of Pile-Soil Interaction," Contract Report No. S-76-14, U.S. Army Corps of Engineers, Waterways Experiment Station, Soil and Pavements Laboratory, September 1976.

27. Holloway, D. M., "Wave Equation Analyses of Pile Driving," Technical Report S-75-5, U. S. Army Corps of Engineers, Waterways Experiment Station, Soils and Pavements Laboratory, June 1975.

28. Holloway, D. M., Audibert, J.M.E., and Dover, A. R., "Recent Advances in Predicting Pile Driveability," Proceedings, 10th Annual Offshore Technology Conference, Houston, Texas, Paper No. 3273, May 1978, pp. 1915-1924.

29. Holloway, D. M., Clough, G. W., and Vesic, A. S., "The Effects of Residual Driving Stresses on Pile Performance Under Axial Loads," Proceedings, Tenth Annual Offshore Technology Conference, Houston, Texas, Paper No. 3306, May 1978.

30. Huff, L. G., "Pile Design Predictions in Sand and Gravel Using In Situ Tests," M.S. thesis, Texas A&M University, College Station, Texas, August 1983.

31. Jansz, J. W., Voitus van Hamme, G.E.J.S.L., Gerritse, A., and Bamer, H., "Controlled Pile Driving Above and Under Water with a Hydraulic Hammer," Proceedings, Eighth Annual Offshore Technology Conference, Houston, Texas, Paper No. 2477, May 1976.

32. Likins, G. E., Jr., "High Tension Stresses in Concrete Piles During Hard Driving," Second Seminar on the Dynamics of Pile Driving, Pile Research Laboratory, University of Colorado, Boulder, March 24-25, 1981.

33. Lowery, L. L., Jr., "Wave Equation Utilization Manual," draft User's Guide for TIDYWAVE, Pile Dynamics, Bryan, Texas, 1976.

34. Lowery, L. L., Jr., Hirsch, T. J., Edwards, T. C., Coyle, H. M., and Samson, C. H., Jr., "Pile Driving Analysis -- State-of-the-Art," Texas Transportation Institute, Piling Behavior Research, Research Report No. 33-13 (Final), Texas A&M University, January 1969.

35. Lowery, L. L., Jr., Hirsch, T. J., and Samson, C. H., Jr., "Pile Driving Analysis -- Simulation of Hammers, Cushions, Piles, and Soil," Texas Transportation Institute, Piling Behavior Research, Research Report No. 33-9, Texas A&M University, August 1967.

36. Matlock, H. and Foo, S.H.C., "Axial Analysis of Piles Using a Hysteretic and Degrading Soil Model," Proceedings, International Conference on Numerical Methods in Offshore Piling, London, May 1979.

37. Olson, R. E. and Flaate, K. S., "Pile-Driving Formulas for Friction Piles in Sand," Journal of the Soil Mechanics and Foundations Division, ASCE, Vol. 93, No. SM6, Proc. Paper 5604, November 1967, pp. 279-296.

38. Ramey, G. E. and Hudgins, A. P., "Sensitivity and Accuracy of the Pile Wave Equation," Ground Engineering, Vol. 10, No. 7, October 1977, pp. 45-47.

39. Rempe, D. M., "Mechanics of Diesel Pile Driving," Ph.D. thesis, University of Illinois at Urbana-Champaign, 1975.

40. Roussel, H. J., "Pile Driving Analysis of Large Diameter High Capacity Offshore Pipe Piles," Ph.D. thesis, Department of Civil Engineering, Tulane University, New Orleans, La., 1979.

41. Samson, C. H., Jr., Hirsch, T. J., and Lowery, L. L., Jr., "Computer Study of Dynamic Behavior of Piling," a paper presented to the 3rd Conference on Electronic Computation, ASCE, Boulder, Colorado, 1963.

42. Smith, E.A.L., "Impact and Longitudinal Wave Transmission," Transactions, ASME, August 1955.

43. Smith, E.A.L., "Pile-Driving Analysis by the Wave Equation," Transactions, ASCE, Vol. 127, Proc. Paper 3306, Part I, 1962.

44. Smith, E.A.L., "What Happens When Hammer Hits Pile," Engineering News Record, September 5, 1957.

45. Smith, I. M., "A Survey of Numerical Methods in Offshore Piling," Numerical Methods in Offshore Piling, The Institution of Civil Engineers, London, 1980.

46. Stevens, R. S., Wiltsie, E. A., and Turton, T. H., "Evaluating Pile Driveability for Hard Clay, Very Dense Sand and Rock," Proceedings, 14th Annual Offshore Technology Conference, Houston, Texas, Vol. 1, Paper No. 4205, May 1982, pp. 465-481.

47. Thompson, C. D., "Quake Values Determined from Dynamic Measurements," Proceedings, International Seminar on the Application of Stress-Wave Theory on Piles, Stockholm, Sweden, June 1980, Edited by H. Bredenberg, A. A. Balkema, Publisher, Rotterdam, 1981, pp. 319-322.

48. Tucker, L. M., "The Behavior of Piles in Cohesionless Soils, M.S. thesis, Texas A&M University, College Station, Texas, December 1983.

49. U.S. Army Corps of Engineers, St. Louis District, "Lock and Dam 26 Replacement," U.S. Government Printing Office, Publication No. 665-156/65, September 1980.

50. Voitus van Hamme, G.E.J.S.L., "Discussion on Survey Paper and Driveability (Papers 1-7)," Numerical Methods in Offshore Piling, The Institution of Civil Engineers, London, May 1979, pp. 171-173.

APPENDIX I

PILE TELLTALES DATA

PILE 1-3A

PILE 1-3B

PILE 1-6

PILE 1-9

PILE 2-5

AXIAL DEFLECTION OF PILE 1-3A AS MEASURED BY STRAIN RODS (inches)

APPLIED LOAD (tons)	AXIAL LENGTH ALONG PILE (feet)						
	0.0	5.9	15.4	24.9	34.4	43.9	53.4
25.000	0.016	0.009	0.008	0.006	0.004	0.001	-0.002
50.000	0.045	0.031	0.024	0.019	0.014	0.010	0.006
75.000	0.092	0.074	0.061	0.051	0.043	0.035	0.028
100.000	0.152	0.131	0.112	0.097	0.084	0.072	0.060
150.000	0.301	0.271	0.234	0.210	0.190	0.172	0.155
200.000	0.508	0.464	0.417	0.384	0.355	0.328	0.302
250.000	1.163	1.109	1.048	1.004	0.964	0.928	0.893
300.000	1.827	1.756	1.681	1.628	1.580	1.535	1.493
325.000	2.674	2.589	2.507	2.448	2.396	2.347	2.309

LOADS IN PILE 1-3A (tons)

APPLIED LOAD (tons)	DEPTH (feet)					
	2.950	10.650	20.150	29.650	39.150	48.850
25.000	0.000	3.631	6.471	8.278	9.724	10.964
50.000	0.000	26.767	17.789	15.473	14.138	13.221
75.000	0.000	44.640	32.362	28.926	26.898	25.484
100.000	0.000	66.272	50.370	45.718	42.936	40.980
150.000	0.000	130.188	82.177	70.379	63.669	59.103
200.000	0.000	164.596	115.428	102.088	94.288	88.882
250.000	0.000	212.661	153.510	137.020	127.302	120.531
300.000	0.000	260.302	187.106	166.782	154.817	146.489
325.000	0.000	286.043	205.702	183.384	170.245	161.097

AXIAL DEFLECTION OF PILE 1-3B AS MEASURED BY STRAIN RODS (inches)

APPLIED LOAD (tons)	AXIAL LENGTH ALONG PILE (feet)						
	0.0	5.9	15.4	24.9	34.4	43.9	53.4
15.000	0.046	0.044	0.040	0.037	0.034	0.032	0.029
30.000	0.145	0.137	0.132	0.126	0.119	0.113	0.107
45.000	0.431	0.420	0.418	0.401	0.392	0.383	0.375
60.000	1.008	0.994	0.980	0.969	0.959	0.949	0.939
66.000	1.631	1.615	1.599	1.587	1.576	1.565	1.555

LOADS IN PILE 1-3B (tons)

APPLIED LOAD (tons)	DEPTH (feet)					
	2.950	10.650	20.150	29.650	39.150	49.650
15.000	0.000	13.726	10.416	9.449	8.872	8.465
30.000	0.000	19.177	20.647	21.241	21.636	21.935
45.000	0.000	35.768	31.844	30.513	29.696	29.676
60.000	0.000	48.207	38.878	35.994	34.240	32.992
66.000	0.000	55.596	42.221	38.311	35.973	34.330

AXIAL DEFLECTION OF PILE 1-6 AS MEASURED BY STRAIN RODS (inches)

APPLIED LOAD (tons)	AXIAL LENGTH ALONG PILE (feet)						
	0.0	10.0	19.5	29.0	38.5	48.0	57.5
50.000	0.054	0.036	0.034	0.022	0.009	0.014	0.012
100.172	0.165	0.140	0.121	0.096	0.075	0.070	0.063
150.000	0.299	0.267	0.231	0.196	0.168	0.158	0.144
200.000	0.435	0.390	0.344	0.296	0.264	0.246	0.230
250.000	0.586	0.529	0.468	0.409	0.372	0.349	0.329
300.000	0.768	0.697	0.619	0.549	0.506	0.475	0.453
350.000	1.026	0.934	0.841	0.757	0.708	0.670	0.644
400.000	1.437	1.324	1.205	1.105	1.048	1.012	0.986

LOADS IN PILE 1-6 (tons)

APPLIED LOAD (tons)	DEPTH (feet)					
	5.000	14.750	24.250	33.750	43.250	52.750
50.000	0.000	6.868	41.211	44.645	17.171	6.868
100.172	0.000	65.250	85.855	72.118	17.171	24.039
150.000	0.000	123.632	120.197	96.158	34.342	48.079
200.000	0.000	157.974	164.842	109.895	61.816	54.947
250.000	0.000	209.487	202.618	127.066	78.987	88.684
300.000	0.000	267.868	240.395	147.671	106.461	75.553
350.000	0.000	319.382	288.474	168.276	130.500	89.289
400.000	0.000	408.671	343.421	195.750	123.632	89.289

AXIAL DEFLECTION OF PILE 1-9 AS MEASURED BY STRAIN RODS (inches)

APPLIED LOAD (tons)	AXIAL LENGTH ALONG PILE (feet)						
	0.0	5.4	15.8	26.1	36.4	46.9	57.2
11.000	0.005	0.006	0.003	0.002	0.002	0.001	0.001
20.000	0.011	0.012	0.007	0.005	0.004	0.003	0.003
30.000	0.020	0.019	0.013	0.007	0.007	0.004	0.004
40.000	0.031	0.028	0.019	0.013	0.011	0.006	0.005
50.000	0.042	0.039	0.029	0.021	0.015	0.013	0.008
100.000	0.133	0.124	0.102	0.082	0.064	0.051	0.043
150.000	0.252	0.239	0.205	0.177	0.144	0.124	0.100
200.000	0.394	0.376	0.330	0.289	0.242	0.215	0.197
250.000	0.585	0.560	0.501	0.449	0.387	0.352	0.329
300.000	1.073	1.030	0.965	0.899	0.817	0.771	0.741

LOADS IN PILE 1-9 (tons)

APPLIED LOAD (tons)	DEPTH (feet)					
	2.700	10.600	20.950	31.250	41.650	52.050
11.000	0.000	9.411	3.167	1.594	1.554	0.808
20.000	0.000	15.695	6.335	3.167	3.107	0.890
30.000	0.000	18.822	19.005	9.839	9.321	0.983
40.000	0.000	28.233	19.005	6.335	15.536	3.167
50.000	0.000	31.370	25.340	19.005	15.536	6.335
100.000	0.000	69.014	63.359	57.015	40.393	25.340
150.000	0.000	106.659	86.689	104.527	62.143	47.512
200.000	0.000	144.393	129.867	148.871	83.993	57.015
250.000	0.000	185.084	167.876	193.216	106.750	72.952
300.000	0.000	232.139	209.053	259.733	142.929	95.024

AXIAL DEFLECTION OF PILE 2-5 AS MEASURED BY STRAIN RODS (inches)

APPLIED LOAD (tons)	AXIAL LENGTH ALONG PILE (feet)						
	0.0	5.5	15.9	26.2	36.5	46.9	57.2
25.000	0.014	0.012	0.008	0.005	0.006	0.003	0.002
50.000	0.038	0.033	0.022	0.016	0.013	0.007	0.006
75.000	0.072	0.063	0.046	0.034	0.026	0.018	0.016
100.000	0.113	0.100	0.077	0.059	0.049	0.038	0.032
125.000	0.184	0.167	0.138	0.113	0.098	0.079	0.076
150.000	0.265	0.246	0.210	0.178	0.159	0.137	0.128
175.000	0.359	0.336	0.293	0.255	0.231	0.206	0.197
200.000	0.651	0.625	0.571	0.528	0.497	0.471	0.457
225.000	1.131	1.101	1.037	0.986	0.954	0.923	0.904

LOADS IN PILE 2-5 (tons)

APPLIED LOAD (tons)	DEPTH (feet)					
	2.750	10.700	21.050	31.350	41.700	52.050
25.000	0.000	12.399	9.390	3.139	9.308	3.130
50.000	0.000	34.098	18.780	9.390	10.509	3.130
75.000	0.000	52.697	37.559	18.789	30.996	6.289
100.000	0.000	71.296	56.339	31.299	40.290	12.529
125.000	0.000	89.895	78.248	46.949	50.997	9.390
150.000	0.000	111.594	109.158	59.469	60.106	20.109
175.000	0.000	133.293	118.938	75.118	77.496	28.109
200.000	0.000	167.391	134.587	97.828	80.596	43.019
225.000	0.000	198.390	153.367	106.418	96.095	59.489

DETERMINATION OF LOAD-DEFORMATION CURVES

Telltales were placed along the entire length of each pile at approximately 10 ft intervals. These telltales recorded axial deflections in the pile for the incremental loads applied during the load test. The axial deflections were used to calculate the loads at each interval along the pile. Axial deflections and back-calculated loads comprise the raw data.

The point load is the load recorded at the maximum depth along the pile, and it is read directly from the raw data. Since the maximum depth is really an average depth between the last two telltale locations, the corresponding point deflection is the average of the last two telltale readings. For pile load test 1-3A, the point load and point deflection due to an applied load of 100 tons are 82.0 kips and 0.066 inches, respectively.

Friction load equals the total applied load minus the point load. The deflection corresponding to the friction load is an interpolated value at the middle of the pile, i.e. it is an average of the shallowest and deepest telltale readings. For pile load test 1-3A, the friction load and average deflection due to a 100 ton applied load are 118.0 kips and 0.106 inches, respectively.

Friction and point loads -- with their corresponding deflections -- were determined for ech increment of applied load for each pile. Plotting these points gave the load-deformation curves used in the analysis (Figs. 35-42).

VITA

William Dieterich Lawson was born on August 25, 1960 in Temple, Texas. He grew up on a ranch and attended a two-room country school for the first six years of his education. He graduated from Belton High School in Belton, Texas in 1978. He received a Bachelor of Science degree in Civil Engineering from Texas A&M University in 1982.

He worked for his father, a self-employed water-well driller, until he started college; during his undergraduate studies he worked at a myriad of jobs ranging from weighmaster at a cotton gin to junior engineer for two consulting engineering firms. During his graduate work, he was a lab instructor for a basic surveying course.

His permanent address is Route #5, Box 225, Temple, Texas, 76501.

"I have acknowledged Christ as the sure foundation of my life. Even more than this, though, Christ is the bright and shining goal of my life - 'a choice stone, a precious cornerstone, and he who believes in Him shall not be disappointed.' (I Peter 2:6, New American Standard Bible).

It is my desire that these few words will lead some to begin to realize that they, too, can have "The Solid Rock" for a foundation, and that they will accept Him as their personal Lord and Savior. Christianity is the only thing in this world that I have found to be unchangeable and totally consistent, and I cannot acknowledge anything apart from Christ. Since Christ is my goal, and the goal is achieved last, I acknowledge Him - at the end - as the end of not only this work, but all things. Christ is '. . . the beginning and the end' (Revelation 22:13, New American Standard Bible)."